

Exploration of Structure–Activity Relationship of Aromatic Aldehydes Bearing Pyridinylmethoxy-Methyl Esters as Novel Antisickling Agents

Piyusha P. Pagare, Mohini S. Ghatge, Qiukan Chen, Faik N. Musayev, Jurgen Venitz, Osheiza Abdulmalik, Yan Zhang* and Martin K. Safo*



Cite This: <https://dx.doi.org/10.1021/acs.jmedchem.0c01287>



Read Online

ACCESS |



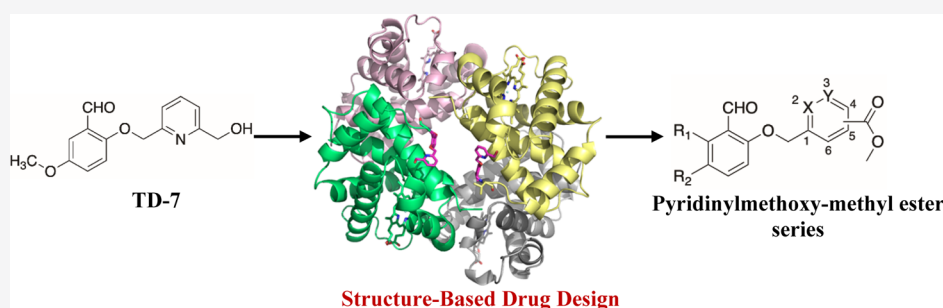
Metrics & More



Article Recommendations



Supporting Information



ABSTRACT: Aromatic aldehydes elicit their antisickling effects primarily by increasing the affinity of hemoglobin (Hb) for oxygen (O₂). However, challenges related to weak potency and poor pharmacokinetic properties have hampered their development to treat sickle cell disease (SCD). Herein, we report our efforts to enhance the pharmacological profile of our previously reported compounds. These compounds showed enhanced effects on Hb modification, Hb-O₂ affinity, and sickling inhibition, with sustained pharmacological effects *in vitro*. Importantly, some compounds exhibited unusually high antisickling activity despite moderate effects on the Hb-O₂ affinity, which we attribute to an O₂-independent antisickling activity, in addition to the O₂-dependent activity. Structural studies are consistent with our hypothesis, which revealed the compounds interacting strongly with the polymer-stabilizing α F-helix could potentially weaken the polymer. *In vivo* studies with wild-type mice demonstrated significant pharmacologic effects. Our structure-based efforts have identified promising leads to be developed as novel therapeutic agents for SCD.

INTRODUCTION

Sickle cell disease (SCD) is an inherited genetic disorder that is caused by a mutation at the sixth position of the β -chain of normal hemoglobin (HbA), which results in substitution of a polar glutamic acid (Glu) residue for a hydrophobic valine (Val) to form sickle Hb (HbS).¹ Under hypoxic conditions, the concentration of the low affinity deoxygenated HbS (deoxyHbS) increases, which polymerizes into long, rigid, and insoluble fibers with concomitant sickling of red blood cells (RBCs). The polymerization process is initiated by a primary interaction between β 2Val6 from one deoxyHbS molecule and a hydrophobic acceptor pocket in the region of β 1Ala70, β 1Phe85, and β 1Leu88 of another deoxyHbS molecule.^{2–4} The polymerization process is further worsened because of high levels of 2,3-diphosphoglycerate present in sickle RBCs, which is an adaptive process to increase tissue oxygenation in SCD patients.^{5–8} The hypoxia-induced RBC sickling leads to multiple secondary pathophysiological events, for example, adhesion of RBCs to tissue endothelium, oxidative stress/damage, hemolysis of RBCs, hemolytic anemia, inflammation, vaso-occlusion, impaired microvascular blood flow, decreased

vascular nitric oxide (NO) bioavailability, painful crises, multi-organ damage, morbidity, and mortality.^{9–11}

Several secondary contacts between the deoxyHbS molecules also play important roles in stabilizing the HbS polymers, as demonstrated by a number of naturally occurring mutations that disrupt these polymer-stabilizing contacts and in turn reduce HbS polymerization and RBC sickling. For example, α Asn78 \rightarrow Lys (Hb Stanleyville) leads to increase in the solubility of deoxyHbS heterotetramers, mitigating the severity of SCD.^{12–14}

Approximately, 100,000 Americans have SCD, and the Centers for Disease Control and Prevention (CDC) has declared this disease as a major public health concern.¹⁵ Four drugs have currently been approved for treating SCD. These

Received: July 23, 2020

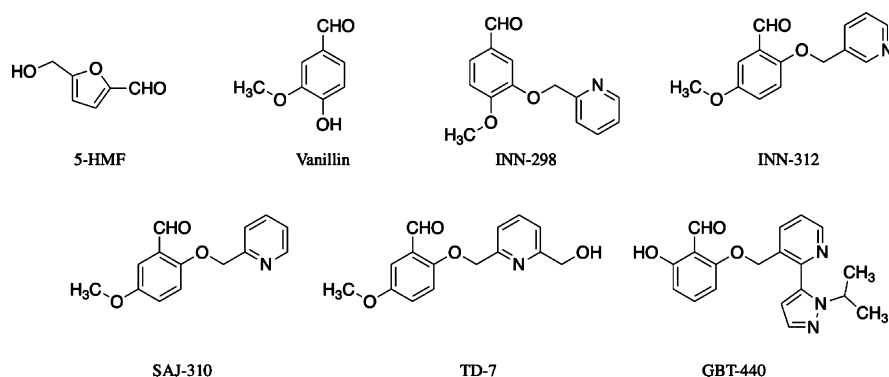


Figure 1. Structures of 5-HMF, vanillin, INN-298, INN-312, SAJ-310, TD-7, and GBT-440.

include hydroxyurea (HU),^{16,17} which has been used for about two decades. There is reported lack of response to HU in up to 30% of patients due to a complex variety of reasons.¹⁸ L-Glutamine (Endari), an antioxidant, was approved in 2017 by the US FDA and expected to reduce painful crises and adverse events;¹⁹ however, the European regulatory body recommended against approval of the medication because of limited evidence of efficacy in phase III trials.²⁰ GBT-440 (Aka Voxelotor or Oxbritya),²¹ (Figure 1), and Crizanlizumab²² were approved in 2019. The latter is a monoclonal antibody targeting P-selectin, to reduce the frequency of painful vaso-occlusive crises. As intracellular polymerization of deoxyHbS remains the principal cause of the pathophysiology-associated SCD, GBT-440, which directly prevents hypoxia-induced RBC sickling by increasing Hb affinity for oxygen, offers immense therapeutic potential.²³ Although, in the clinic, GBT-440 showed proof-of-principle disease-modifying potential by increasing Hb levels and reducing hemolysis in patients, there was no evidence of efficacy against vaso-occlusion. Thus, there is a need for novel aromatic aldehydes for treating SCD with better clinical outcomes.

Prior to GBT-440, several aromatic aldehydes were studied as allosteric effectors of hemoglobin (AEHs) for their antisickling activities.^{24,25} Specifically, these compounds form Schiff-base adducts with the Val1 amines of both α -subunits of Hb increase Hb-O₂ affinity and ameliorate the primary pathophysiology of SCD, that is, RBC sickling. Several challenges relating to the application of aromatic aldehydes for treating SCD became apparent during the early years of their development. These include nonspecific binding to plasma proteins and susceptibility of the active aldehyde moiety to rapid oxidative metabolism by several enzymes, for example, aldehyde oxidase (AO) and aldehyde dehydrogenases (ALDHs),^{26–32} that compromise the effectiveness of these compounds dramatically. Another major challenge is the difficulty in designing pharmaceutically applicable agents that are capable of sustained modification of the large amounts of intracellular Hb (~5 mmol) in the body. These problems led to termination of clinical trials of vanillin and 5-HMF (Aes103)²⁹ for SCD. GBT-440 appeared to have overcome some of these problems. While the long-term benefits of GBT-440 are still unclear, the need remains critical for additional investigations into strategies to further enhance this class of compounds. In our continuous efforts to develop aromatic aldehydes for SCD, we have adopted a structure-based approach to modify the antisickling agent, vanillin, resulting in several generations of potent, allosteric, and covalent-binding antisickling derivatives.^{33–39} From vanillin to the

INN³³ or SAJ³⁹ series and then to TD³⁵ series of compounds (Figure 1), significantly improved antisickling activities have been observed. Among these, the INN and SAJ compounds are pyridyl derivatives of vanillin, while the TD compounds represent further modifications of the INN compounds (with a hydroxymethyl group on the pyridine ring) rationalized to stereospecifically inhibit deoxyHbS polymer formation by perturbing the α F-helix and contribute to the antisickling activity of the compounds through the O₂-independent antisickling mechanism. At every stage, co-crystallization of these compounds in complex with Hb revealed insights into their binding and guided our future structure-based modifications. These compounds, however, still underwent significant metabolism leading to suboptimal pharmacokinetics properties, for example, short duration of action and low bioavailability, mainly because of the highly susceptible aldehyde pharmacophore. Nonetheless, the development of vanillin,⁴⁰ 5HMF,^{38,41} and GBT-440⁴² demonstrated that these allosteric modulators of Hb carry no significant toxicity even at high doses and thus established aromatic aldehydes as a scaffold to design potential therapeutics for SCD.

In this current work, we aimed to design a series of aromatic aldehydes that potentially improve the antisickling activity of aromatic aldehydes while addressing some of the challenges associated with the rapid metabolism of the aldehyde pharmacophore.

RESULTS AND DISCUSSION

Molecular Design. Two molecules of vanillin bind to the α -cleft of Hb in a symmetry-related fashion, forming Schiff-base interactions with the N-terminal amines of the two α -subunits. Our previous studies identified several vanillin derivatives, for example, SAJ-310,³⁹ INN-312,³⁴ and INN-298³⁴ (Figure 1) with improved *in vitro* antisickling potency compared to vanillin.³⁵ Some of these compounds, for example, INN-312 with the pyridinylmethoxy substitution ortho to the aldehyde group, showed a second novel O₂-independent antisickling activity, although weak, which was attributed to weak hydrophobic interactions with a surface-located α F-helix. Based on structural studies, we subsequently modified the SAJ and INN series of compounds to generate another series of compounds termed TD, by incorporating the hydroxymethyl group on the pyridine ring. The rationale was to increase protein interactions with the α -cleft residues to potentially increase Hb oxygen affinity (O₂-dependent antisickling activity), as well as strongly interact with the surface-located α F-helix to directly weaken polymer interactions (O₂-

independent antisickling activity). The most promising compound, TD-7, however undergoes significant metabolism leading to suboptimal pharmacokinetics properties, for example, short duration of pharmacologic action and low bioavailability. In addition, the co-crystal structure of TD-7 with Hb revealed that the hydroxymethyl group did not make interactions with the α F-helix as anticipated.³⁵ Therefore, we decided to pursue further structure-based modifications to design better pharmacological agents.

In the current study, we structurally modified TD-7 by first replacing the hydroxymethyl group on the pyridine ring with a methyl ester group, as well as varying its position on the pyridine ring while maintaining the *meta*-methoxy on the benzaldehyde ring (Table 1, compounds 1–7). Introduction of

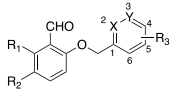
lization and/or increase interactions with Hb to improve both the O₂-independent and O₂-dependent antisickling activities. Next, to reduce oxidative metabolism of the aldehyde moiety, we introduced an *ortho*-hydroxy group on the benzaldehyde ring (Table 1, compounds 8–14). As previously observed, the *ortho*-hydroxy is expected to form an intramolecular hydrogen-bond interaction with the aldehyde moiety to reduce enzymatic metabolism.^{43,44}

In summary, two series of compounds, one with the 5-methoxy group (1–7) and second with the 2-hydroxy group (8–14) on the aromatic aldehyde ring, were synthesized, as shown in Table 1. Each series contained 2- and 3-pyridine-substituted benzaldehydes with the methyl esters at different positions on the pyridine ring. Because of unavailability of reagents as well as limitations in the synthetic feasibility, the 4-substituted pyridine derivatives were not included.

Chemistry. All target compounds in Table 1 were synthesized in two steps. The first step was a radical-catalyzed Wohl–Ziegler bromination reaction of a methyl-substituted pyridylmethyl ester to give bromomethyl-substituted pyridylmethyl ester. The starting materials used for these reactions were commercially available methyl-substituted methyl esters of nicotinic acid and picolinic acid. *N*-Bromosuccinimide (NBS) was used as the brominating agent, while 2,2'-azobis(2-methylpropionitrile) (AIBN) was applied as the radical initiator. The bromomethyl pyridine intermediates obtained were then used to form an ether linkage between the phenolic oxygen of either 2-hydroxy-5-methoxybenzaldehyde or 2,6-dihydroxybenzaldehyde via Williamson's synthesis using the previously reported procedure (Scheme 1).^{35,39} The synthesis of TD-7, as a positive control, has been reported.^{33,39} The compounds were obtained in reasonable yields (75–90%), fully characterized, and then investigated for binding interactions with Hb, as well as *in vitro* and *in vivo* pharmacokinetics and/or pharmacodynamics (PDs) studies using normal and sickled blood or wild-type mice.

Compounds Potently Increase Hb Affinity for Oxygen. Aromatic aldehydes are known to bind to Hb allosterically and modify it, either to increase its O₂ affinity [stabilizing the relaxed (R) state] or increase O₂ delivery [stabilizing the tense (T) state].^{25,45–50} Increasing the Hb-O₂ affinity is the primary mechanism by which these compounds elicit antisickling effects as the R-state Hb is resistant to polymerization. Thus, oxygen equilibrium curve (OEC) studies were first conducted using normal human whole blood to determine the effects of the compounds on Hb's affinity for oxygen.

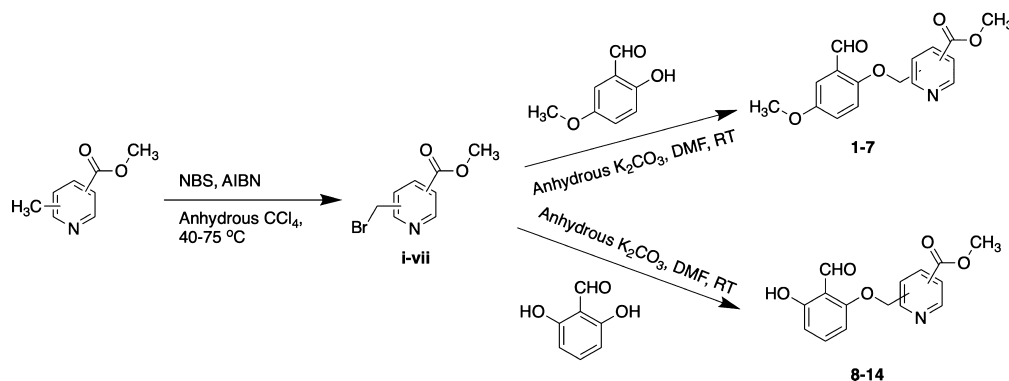
Table 1. Structures of Target Compounds



Compd.	R ₁	R ₂	X	Y	R ₃
1	H	-OCH ₃	N	CH	4- 
2	H	-OCH ₃	N	CH	6- 
3	H	-OCH ₃	N	CH	3- 
4	H	-OCH ₃	N	CH	5- 
5	H	-OCH ₃	CH	N	2- 
6	H	-OCH ₃	CH	N	4- 
7	H	-OCH ₃	CH	N	5- 
8	-OH	H	N	CH	4- 
9	-OH	H	N	CH	6- 
10	-OH	H	N	CH	3- 
11	-OH	H	N	CH	5- 
12	-OH	H	CH	N	2- 
13	-OH	H	CH	N	4- 
14	-OH	H	CH	N	5- 

the methyl ester group was expected to lead to closer interactions with the α F-helix and increase polymer destabi-

Scheme 1. Synthetic Route for Target Compounds



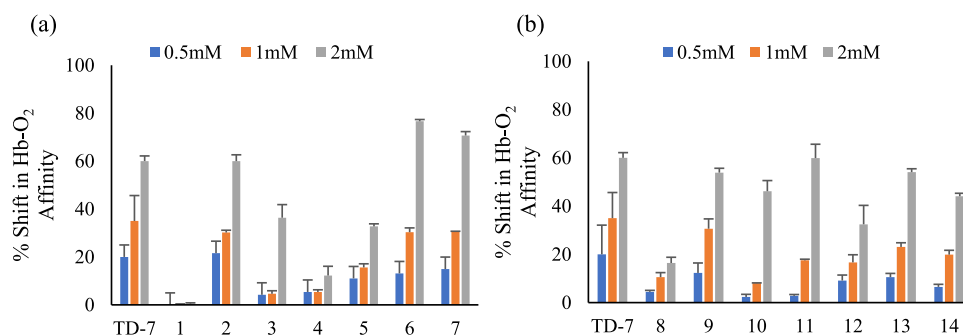


Figure 2. Concentration-dependent shift in the Hb-O₂ affinity of (a) *m*-methoxy-substituted and, (b) *o*-hydroxy-substituted compounds in normal whole blood after 1.5 h incubation.

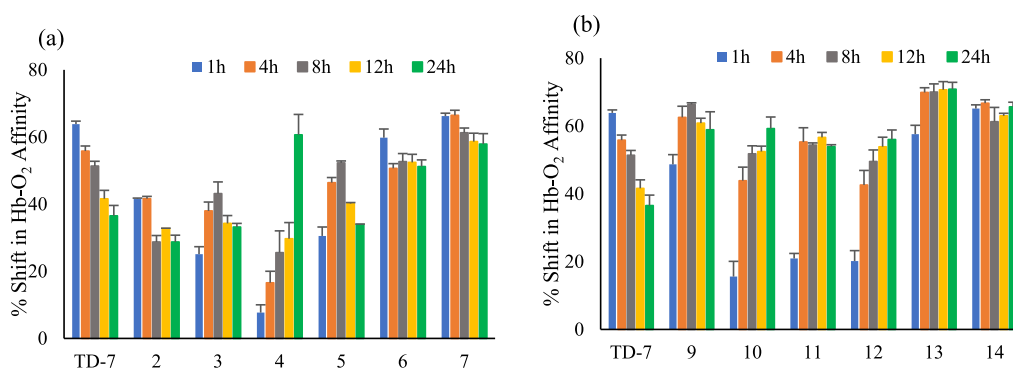


Figure 3. Time-dependent shift in the Hb-O₂ affinity of (a) *m*-methoxy-substituted and, (b) *o*-hydroxy-substituted compounds in normal whole blood at a concentration of 2 mM.

Dose-dependent studies were carried out using 0.5, 1, and 2 mM concentrations of the compounds and normal whole blood (hematocrit adjusted to 30%) at 37 °C as previously reported.³³ The concentration of Hb in blood (~5.0 mmol) warrants the use of such high concentrations of the tested compounds. Whole blood comprises of plasma proteins, enzymes, and RBC cell membrane, which may play an interfering role on the activity of the compounds as compared to purified Hb. Thus, whole blood was used in this study to obtain results more representative of the native system.

As shown in Figure 2, the compounds increased Hb affinity for O₂ in normal whole blood to varying degrees. The low or insignificant activity shown by compounds 1 and 8 was likely because of their low solubility in most solvents, including dimethyl sulfoxide (DMSO). Thus, compounds 1 and 8 were not studied further. The low activity of compounds 3, 5, 10, and 12 compared to TD-7 could be due to the low intrinsic affinity for Hb or due to plasma protein binding and/or difficulty in RBC membrane permeation. It could also be due to significant metabolism by enzymes in the blood and/or RBCs that are known to play deteriorating roles in the bioavailability and potency of antisickling aromatic aldehydes.^{26,29,30,41} In comparison, compounds 2, 6, 7, 9, 11, and 13 showed significant increase in the Hb-O₂ affinity. Vanillin, at 2 mM concentration, only increased Hb O₂ affinity by 21%,³³ whereas TD-7 showed almost similar potency as most of the best compounds. These observations confirmed that the structural modifications have conserved the potent Hb-O₂ affinity *in vitro* activity previously observed in TD-7, the parent lead.

As pointed out above, aromatic aldehydes are highly susceptible to oxidative metabolism of the active aldehyde

function,^{26–30} resulting in most of these compounds having poor oral bioavailability, which has stymied their development. Therefore, one of the major objectives of this work was to identify compounds that may be less susceptible to the oxidative metabolism of the aldehyde pharmacophore. For this reason, time-dependent Hb-O₂ affinity studies were conducted with 2 mM concentrations of the compounds with human blood (hematocrit adjusted to 30%) at 37 °C for 24 h using TD-7 as control. Although, oxidative metabolism of aldehydes occurs by several enzymes in various tissues including AO,^{31,32} it is primarily by ALDH in RBCs;^{26–28} therefore, whole blood serves as an appropriate matrix for the measure of oxidative metabolism *in vitro*. Among the *meta*-methoxy derivatives, compound 2 showed optimal activity between 1 and 4 h which then decreased to about 70% of its activity by 8 h and sustained through the 24 h. Compounds 3 and 5 showed maximum potency at 8 h followed by a gradual decrease over the course of 24 h to about 70 and 60% of its original activity, respectively. Interestingly, three of the *meta*-methoxy derivatives, including compounds 4, 6, and 7 appear to be stable against oxidative metabolism in whole blood. Compound 4 shows a very slow onset and reached its highest potency at 24 h. Such a slow onset may not be optimal because other metabolizing enzymes, such as in the liver, could deactivate this compound before reaching therapeutic potency. Compounds 6 and 7, on the other hand, have quick onset and showed a sustained effect during the 24 h experiment (Figure 3a). In comparison, TD-7, similar to some of the *meta*-methoxy derivatives, also after reaching a maximal effect at 1 h gradually decreased in potency, and at 24 h, showed a loss of almost 45% of its activity. Clearly, the *meta*-methoxy-substituted derivatives show varying oxidative metabolism in whole blood and/or

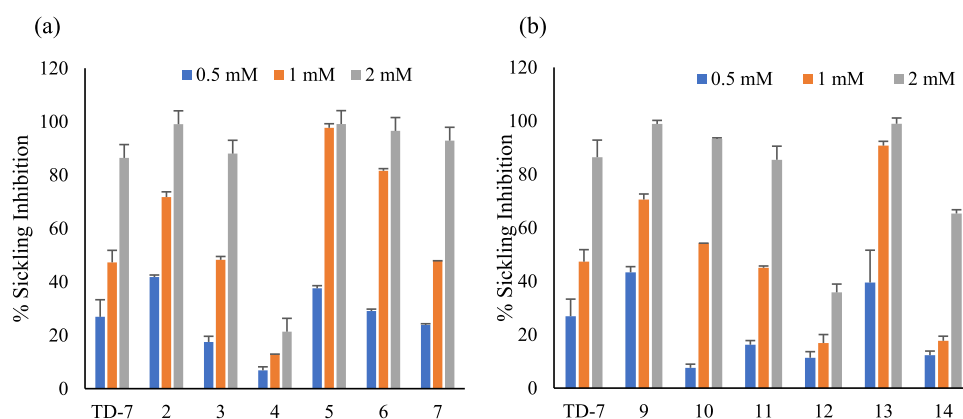


Figure 4. Inhibition of sickling by (a) *m*-methoxy-substituted and, (b) *o*-hydroxy-substituted compounds in SS RBCs.

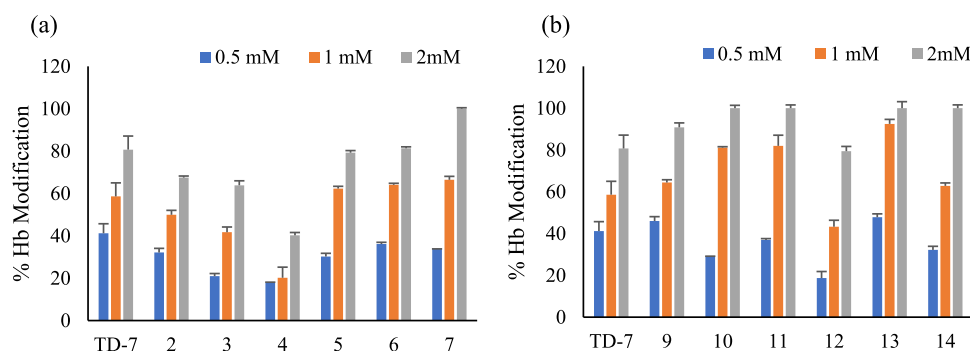


Figure 5. Concentration-dependent Hb modification (adduct formation) by (a) *m*-methoxy-substituted and, (b) *o*-hydroxy-substituted compounds in SS RBCs.

RBC, probably because of differences in their affinity to the metabolizing enzymes, ALDH. What is not clear is whether, when administered *in vivo*, compounds 4, 6, and 7 would still maintain their resistance to oxidative metabolism of the aldehyde.

Unlike the *meta*-methoxy-substituted compounds (Figure 3a), all the *ortho*-hydroxy-substituted compounds (Figure 3b) showed sustained action over the duration of the experiment, suggesting all compounds are resistant to oxidative metabolism in whole blood. Interestingly, compounds 10, 11, and 12 showed relatively slow onset of action compared to the other compounds, which we speculate to be due to slow RBC membrane permeation. As previously reported, formation of intramolecular hydrogen bonding between the aldehyde carbonyl group and the *ortho*-hydroxy group acts as a protection to prevent undue metabolism of the aldehyde.^{43,51} It is clear from the foregoing that not only did we maintain the Hb-O₂ potencies of these compounds but also achieved one of our primary objectives of increasing the metabolic stability of the aldehyde moiety.

The compounds have a major effect of Hb cooperativity as the shape of the OEC changed from sigmoidal to hyperbolic with addition of the compound (Supporting Information S1), as a result of the stabilization of the R-state Hb and restraining the cross talk between the Hb subunits that is important for the R → T transition.^{24,25}

Compounds Potently Increase *In Vitro* Antisickling, Hb-Modification, and Hb-O₂ Affinity Activities with Sick RBCs. Because the pathophysiology of SCD, including RBC sickling, is driven by hypoxia-induced polymerization of deoxyHbS, we further characterized these high-O₂ affinity

compounds for their O₂-dependent antisickling properties. We incubated the compounds at 0.5, 1.0, and 2.0 mM concentrations with blood from individuals with homozygous SS (hematocrit 20%), under hypoxic conditions (2.5% O₂/97.5% N₂) at 37 °C for 2 h. The concentration-dependent antisickling effect was observed for most of the tested compounds (Figure 4). Although compounds 4, 12, and 14 showed dose-dependent sickling inhibition, their antisickling effects were significantly weaker when compared to the other compounds. At a lower concentration of 0.5 mM, compounds 2, 5, 9, and 13 showed more than 35% sickling inhibition as compared to only 26% by TD-7. At 1.0 mM concentration, compounds 5, 6, 9, and 13 showed more than 70% inhibition as compared to 47% by TD-7, with compounds 5 and 13 almost exhibiting 100% sickling inhibition (Figure 4a,b). At 2.0 mM concentration, several of the tested compounds showed more than 90% sickling inhibition.

This observation clearly indicates that the structural modifications have led to improvement in increasing the antisickling potencies of the compounds when compared to TD-7. In comparison, GBT-440 at 0.5 and 1.0 mM decreased the O₂-dependent sickling by 56% and 98%, respectively, suggesting that at lower concentration, GBT440 shows better potency. This enhanced potent activity of GBT-440 has been suggested to be because of reduced binding stoichiometry, that is, it binds Hb at a 1:1 ratio⁵² while our compounds bind Hb at a 2:1 ratio.

The remarkable enhanced antisickling activity of the compounds compared to TD-7 led us to investigate whether such an improvement is solely the consequence of their ability to bind Hb and modify it to the higher O₂ affinity form.

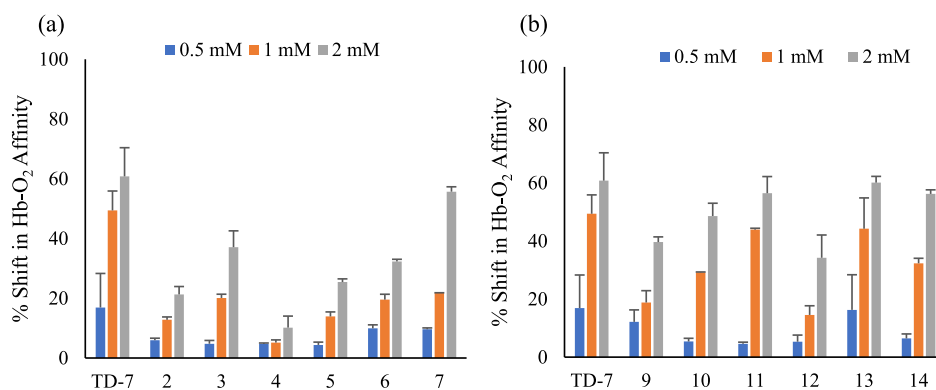


Figure 6. Concentration-dependent shift in Hb-O₂ affinity by (a) *m*-methoxy-substituted and, (b) *o*-hydroxy-substituted compounds in SS RBCs.

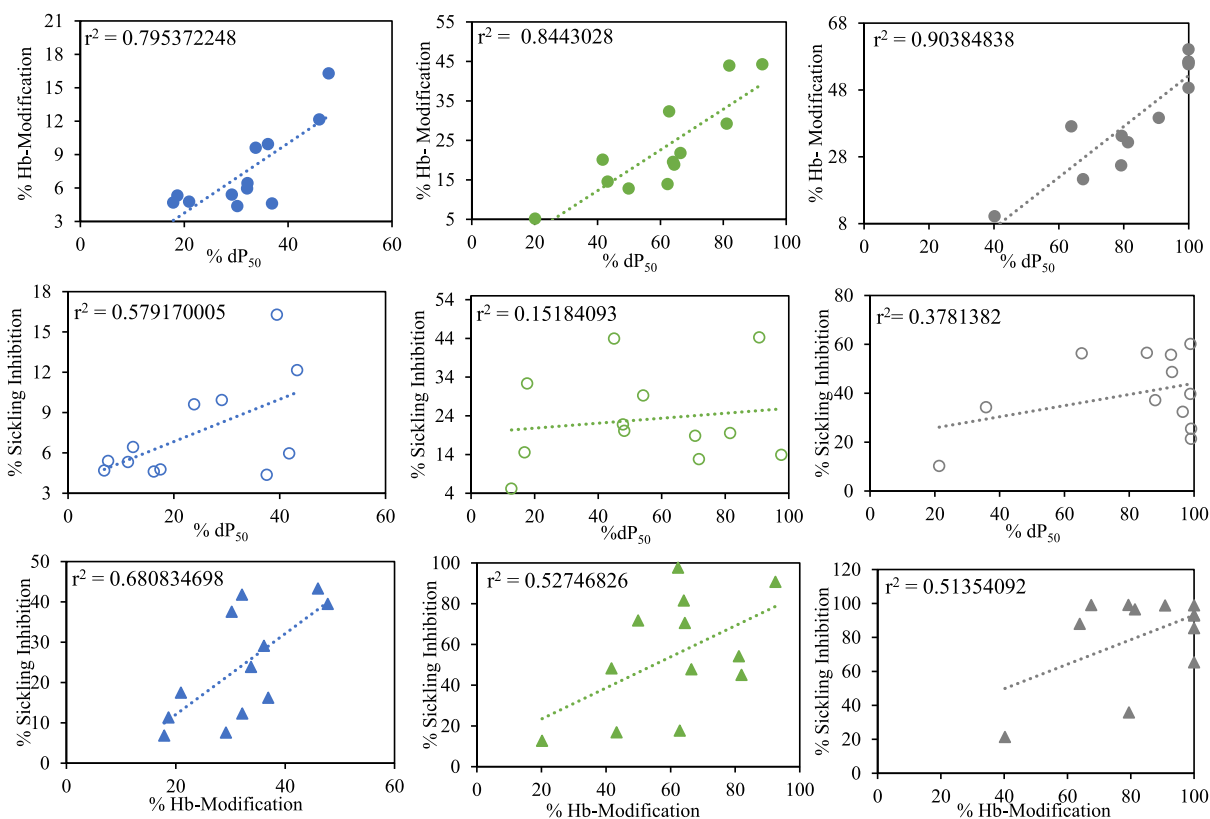


Figure 7. Linear correlation between increase in the Hb-O₂ affinity, antisickling, and Hb-modification properties for 0.5 mM (blue), 1 mM (green), and 2 mM (gray) concentrations of compounds.

Aliquot samples from the above antisickling study were hemolyzed and utilized for dose-dependent Hb-O₂ affinity and Hb modification studies. As observed with normal whole blood (Figure 2), the compounds increased Hb affinity for oxygen and Hb modification in dose-dependent fashions (Figure 5). The modification effect by the compounds were in most instances similar or better than observed with TD-7. For example, compounds 7, 9, 10, 11, 13, and 14 showed almost complete modification of HbS at 2.0 mM concentration compared to the ~80% by TD-7. At 1.0 mM concentration, compounds 5, 6, 7, 9, and 14 modified HbS similar to TD-7 (~60%), while compounds 10, 11, and 13 showed more than 80% HbS modification at the same concentration (Figure 5). In few instances, such as with compounds 2, 3, 4, and 12, TD-7 showed better a Hb modification effect. Interestingly, while compounds 4 and 12 expectedly showed weaker antisickling

effects than TD-7, compounds 2 and 3 appear to show comparable or stronger antisickling effects when compared to TD-7. In comparison, GBT-440 as expected from its potent antisickling activity showed very high Hb modification to the high affinity adduct form of 55% (0.5 mM) and 100% (1.0 mM).

Of most interest is that despite the fact that most of these compounds, with the exception of 4, 12, and 14, show better antisickling effects than TD-7, they conversely increase Hb affinity for oxygen to a lesser degree when compared to TD-7 (Figures 4 and 6). Similar to TD-7, GBT-440's high antisickling activity (56% and 98% at 0.5 and 1.0 mM) also corresponded to very high P_{50} shifts of 41 and 80%, respectively. The unusual weak correlation between the antisickling and P_{50} shift of our newer derivative compounds

Table 2. Sickling Inhibition, Hb-O₂ Affinity, and Hb-Modification Studies Using SS RBCs with the Seven Compounds

compd	% sickling inhibition			% Hb-O ₂ affinity			% Hb-modification		
	0.5 mM	1 mM	2 mM	0.5 mM	1 mM	2 mM	0.5 mM	1 mM	2 mM
2	41.8 ± 0.7	71.7 ± 0.9	99 ± 2.6	5.9 ± 0.7	12.8 ± 1.9	21.3 ± 2.1	32.1 ± 0.5	49.9 ± 1.6	67.5 ± 2.2
3	17.5 ± 1.1	48.2 ± 1.2	88 ± 5.5	4.8 ± 2.1	20.1 ± 1.3	37.1 ± 2.5	20.9 ± 1.5	41.7 ± 1.8	63.8 ± 3.2
5	37.6 ± 0.9	97.7 ± 1.5	99.1 ± 1.1	4.4 ± 0.9	13.9 ± 1.5	25.4 ± 1.1	30.2 ± 0.5	62.3 ± 1.9	79.2 ± 0.6
6	29.1 ± 1.2	81.6 ± 1.8	96.5 ± 0.7	9.9 ± 0.7	19.5 ± 0.8	32.3 ± 0.7	36.1 ± 1.1	64 ± 1.3	81.3 ± 1.4
9	43.3 ± 4.1	70.6 ± 4.1	98.8 ± 1.8	12.2 ± 2.1	18.8 ± 2.1	39.6 ± 1.3	46 ± 3.2	64.4 ± 2.7	90.8 ± 1.2
10	7.6 ± 1.1	54.2 ± 0.1	93.2 ± 4.4	5.4 ± 1.4	29.2 ± 1.1	48.6 ± 0.4	29.2 ± 1.6	81.1 ± 0.6	100 ± 0.7
13	39.5 ± 12	90.7 ± 11	98.9 ± 2.1	16.3 ± 12	44.2 ± 1.6	60.1 ± 2.1	47.8 ± 4.6	92.5 ± 5	100 ± 1.1

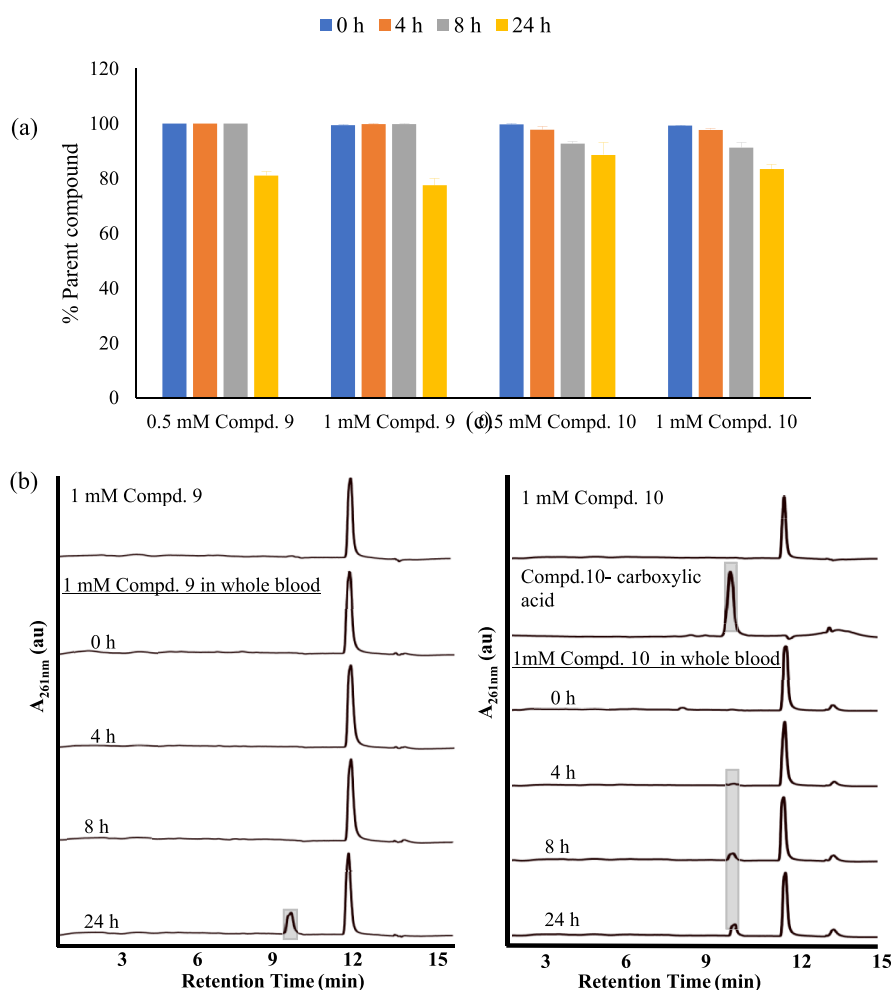


Figure 8. Time-dependent recovery of parent compounds 9 and 10 at 0.5 and 1 mM; (a) representative chromatograms of 1 mM compound 9 and (b) compound 10 at 0, 4, 8, and 24 h.

as discussed below is likely because of a second mechanism of O₂-independent antisickling activity.

The pharmacologic properties of aromatic aldehydes, including their ability to modify Hb, increase Hb affinity for oxygen, and inhibit hypoxia-induced RBC sickling are known to be highly correlated. For example 5-HMF, when incubated with sickle blood results in perfect direct correlations ($r^2 = 1$) between any two of the biological parameters, that is, Hb adduct, P_{50} shift, or sickling inhibition.⁴¹ With the newer derivative compounds, even though we observed a relatively good correlation between the Hb adduct and P_{50} shift ($r^2 = 0.8-0.9$) (Figure 7), it is weaker than reported for 5-HMF⁴¹ or GBT-440. Even more so, the correlation between antisickling activity and Hb modification are weaker and especially

between antisickling activity and P_{50} shift (Figure 7). The weak correlation between the PD parameters of the compounds presented here clearly suggests additional unique mechanism of antisickling action that is particularly independent of Hb oxygen affinity. Compounds 2, 3, 5, 6, 9, 10, and 13 demonstrated the most potent antisickling effects despite only marginally increasing Hb affinity for oxygen (Figure 7, Table 2). For example, while compound 9 inhibits sickling and increases Hb-O₂ affinity by 43 and 12% at 0.5 mM (71 and 19% at 1.0 mM), respectively, GBT-440 on the other hand inhibits sickling and increases Hb oxygen affinity by 56 and 41%, at 0.5 mM (100 and 80% at 1 mM), respectively. This substantial antisickling activity, but at a relatively much lower Hb-O₂ affinity increase by some of our compounds, were

propose, is because of the polymer destabilization effect that potentially led to an O₂-independent antisickling activity contribution, which is currently under further investigation.

Stability Studies of Compounds Using Whole Blood Show Limited Hydrolysis of the Parent Methyl Ester.

The parent compounds reported here contain the methylester moiety, which could potentially hydrolyze into their corresponding acids and affect the PK or PD properties. We therefore studied representative compounds, **9** and **10**, for their stability in buffer and whole blood using reversed-phase high-performance liquid chromatography (HPLC). The compounds at 0.5 and 1 mM concentrations were incubated in normal whole blood (hematocrit adjusted to 30%) at 37 °C, and aliquots obtained at 0, 4, 8, and 24 h were subjected to deproteinization and extraction of the compounds in organic solvent (acetonitrile). The purified extracts were subjected to HPLC analyses to detect and quantify the amount of the parent compound present, as well as any metabolized derivatives. The acid analogue of compound **10** was used as a control, which as expected eluted before the parent compound (Figure 8). Both parent compounds showed formation of the carboxylic acid analogue, but at very low levels (Figure 8). Compound **10** demonstrated a time-dependent hydrolysis of the methyl ester to the acid analogue, with 89 ± 4.4% (0.5 mM) and 83 ± 1.7% (1 mM) of parent compound **10** retained at 24 h (Figure 8a,c). Interestingly, compound **9** did not show any observable metabolism until 24 h, with 81 ± 1.4% (0.5 mM) and 78 ± 2.4% (1 mM) of the parent compound **9** being retained (Figure 8a,b). Thus, during the course of 24 h, only approximately 20% of compounds **9** and **10** metabolized into the carboxylic acid form, indicating that the antisickling activity of both compounds (and in general all compounds) which were conducted within 3 h of experimentation is likely exclusively due to the parent methyl esters.

X-ray Crystallography Shows Compounds Bind as Predicted and Provide Atomic Basis for Their Potent Antisickling Activities. To verify our molecular design, which was intended toward these compounds interacting with the α F-helix of Hb, as well as explain the unusual functional/biological effects of the compounds, we selected two compounds, one each from the *meta*-methoxy-substituted and *ortho*-hydroxy-substituted benzaldehyde series, namely, compounds **6** and **9** respectively, for co-crystallization studies with CO-liganded Hb (COHb) in the R2-state conformation. COHb was used for the crystallographic study because the structures of O₂-Hb and COHb complexes are very similar, while the latter is comparatively easy to purify, more stable, and easier to work with. Also, normal Hb (HbA) instead of HbS was used for the crystallographic study because the quaternary structures as well as the size and geometry of the α -cleft binding site are similar in the two Hb structures.^{4,52} Freshly made solution of the compounds was added to deoxygenated Hb (30 mg/mL protein) at an Hb tetramer-compound ratio of 1:10. The complex mixture was saturated with CO and allowed to incubate for 2 h to form the COHb-compound complex. Co-crystallization experiments were carried out under low salt precipitant conditions (10–20% PEG6000, 100 mM HEPES buffer, pH 7.4), where cherry red needle crystals, isomorphous to previous aromatic aldehyde Hb-R2 state complex crystals, appeared in 1–3 days and were used to collect X-ray diffraction data.^{35,39} The crystal structures of the COHb complexes with compounds **6** and **9** were

determined by the molecular replacement method with the Phenix program⁵³ using the native R2-state crystal structure (PDB ID 1BBB) as a search model. Structure refinement was carried out using both Phenix and CNS,⁵⁴ and model correction was carried out using COOT.⁵⁵ The crystal structures of COHb-**6** (PDB ID 6XDT) and COHb-**9** (PDB ID 6XE7) complexes were refined to 1.9 and 2.0 Å, respectively. The overall tetrameric structures of both complexes were indistinguishable from 1BBB (RMSD 0.3 Å), and their detailed crystallographic data are summarized in Table 3.

Table 3. Crystallographic Data and Refinement Statistics for COHb-6 and COHb-9 Complexes

compound	6 (PDB ID6XDT)	9 (PDB ID6XE7)
Data Collection Statistics		
space group	P2 ₁ 2 ₁ 2 ₁	P2 ₁ 2 ₁ 2 ₁
unit-cell <i>a</i> , <i>b</i> , <i>c</i> (cÅ)	63.68, 82.98, 105.03	62.64, 82.76, 104.77
resolution (cÅ)	29.32–1.90 (1.97–1.90)	29.29–2.00 (2.07–2.00)
unique reflections	40,600 (3764)	37,109 (3683)
redundancy	4.27	4.04
completeness (%)	92.5 (86.9)	98.9 (99.7)
average <i>I</i> / σ (<i>I</i>)	13.4 (3.3)	8.5 (2.3)
<i>R</i> _{merge} (%) ^a	5.5 (37.3)	7.9 (42.8)
Refinement Statistics		
resolution (cÅ)	30.00–1.90	30.00–2.00
no. of reflections	40,573	37,580
<i>R</i> _{work} (%)	18.81	19.94
<i>R</i> _{free} (%) ^b	23.91	25.14
rmsd bonds (cÅ)	0.006	0.006
rmsd angles (deg)	0.97	0.83
Dihedral Angles		
most favored (%)	98.00	98.00
allowed (%)	1.78	1.96
Average <i>B</i> (cÅ ²)/Atoms		
all atoms	32.00	34.90
protein	31.50	34.40
ligand	29.50	35.00
water	36.90	39.00

^a*R*_{merge} = $\sum_{hkl} \sum_i |I_i(hkl) - \langle I(hkl) \rangle| / \sum_{hkl} \sum_i I_i(hkl)$. ^b*R*_{free} was calculated from 5% randomly selected reflection for cross-validation. All other measured reflections were used during refinement.

As expected, compounds **6** and **9** bind in a symmetry-related fashion, forming Schiff base interactions between the aldehyde group of the compounds with the α Val1 nitrogens (~1.5 cÅ) of both α 1- and α 2-subunits at the α -cleft of Hb. Also, as anticipated, the *ortho*-substituted pyridinylmethoxy-methyl ester groups directed upward toward the surface of the α -cleft and close to the α F-helix (Figures 9 and 10). Because both molecules in their respective structures bind in a symmetrical fashion, detailed interaction analyses with Hb will be focused on α 2Val1 binding, which appears to be more ordered than the α 1Val1 binding, especially with compound **9**.

The benzaldehyde ring of both compounds **6** and **9** superimposed closely, making both intra- and inter-subunit hydrophobic interactions with α 2Ala130, α 2Ser131, α 2Thr134, and α 1Thr134 (Figures 9–11). The pyridine rings of the two bound molecules formed extensive face-to-face π - π stacking interactions (3.4–3.8 cÅ) (Figures 9 and 10). These interactions serve to stabilize the R-state and increase the oxygen affinity of Hb, as reported previously.²⁵

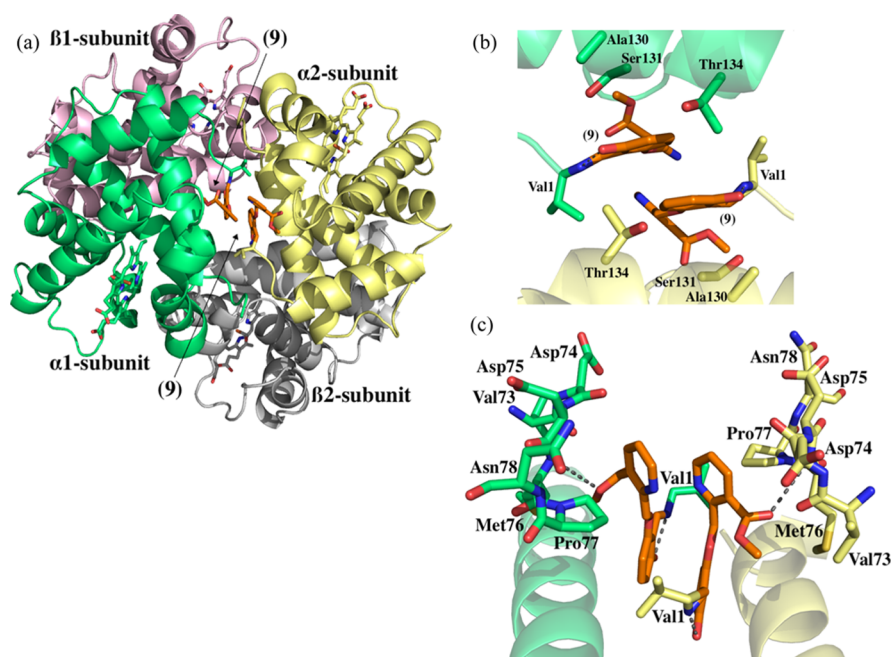


Figure 9. Crystal structure of Hb in the R2 conformation in complex with two molecules of compound 9 bound at the α -cleft (a) overall crystal structure of Hb in the R2 conformation in the complex with two molecules of compound 9 in the central water cavity. (b) Close-up view of compound 9 bound at the α -cleft of Hb. (c) Close-up view of compound 9 showing interactions with the residues of the α F-helix. (Hb is shown as cartoon with α 1 subunit in green, α 2 in yellow, β 1 in pink, and β 2 in gray; hemes are shown as sticks; compound 9 is shown in orange sticks).

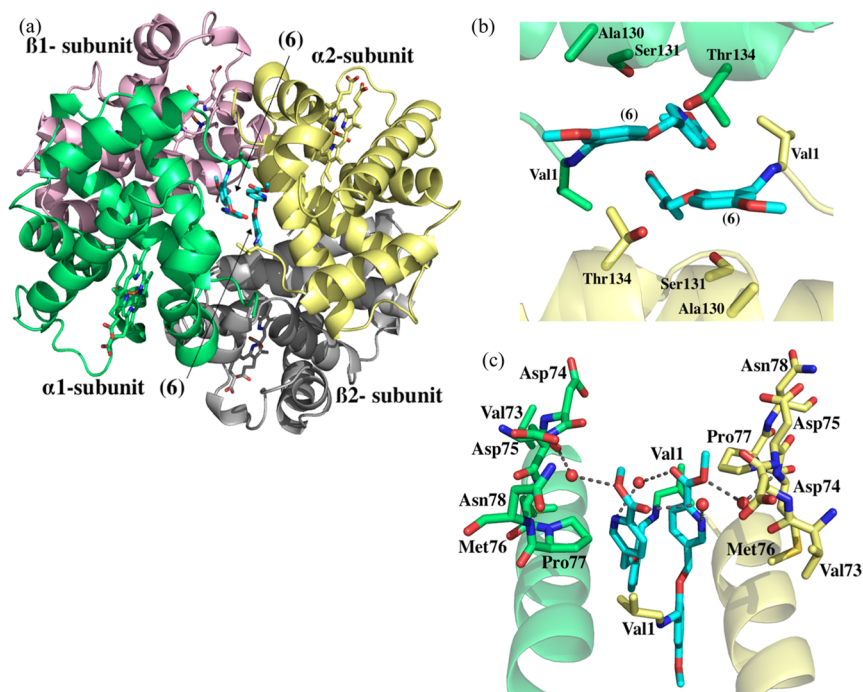


Figure 10. Crystal structure of Hb in the R2 conformation in complex with two molecules of compound 6 bound at the α -cleft (a) overall crystal structure of Hb in the R2 conformation in complex with two molecules of compound 6 in the central water cavity. (b) Closeup view of compound 6 bound at the α -cleft of Hb. (c) Closeup view of compound 6 showing interactions with the residues of the α F-helix. (Hb is shown as cartoon with α 1 subunit in green, α 2 in yellow, β 1 in pink, and β 2 in gray; hemes are shown as sticks; compound 6 is shown in cyan sticks; water molecules are shown as red spheres).

Interestingly, the *ortho*-hydroxy group of compound 9 makes both direct and water-mediated hydrogen bonding interactions with the α Val1 nitrogen. This interaction may help increase the binding affinity of compound 9 with the protein (Figure 3). The pyridinylmethoxy-methyl ester group in compound 9,

which is directed toward the surface of the α -cleft, is involved in a hydrogen bonding interaction with the backbone nitrogen of α 2Met76 of the α F-helix (3.5 c5) (Figure 9), which is missing in TD-7 binding.³⁵ In addition, the pyridinylmethoxy-methyl ester group is also involved in hydrophobic interactions

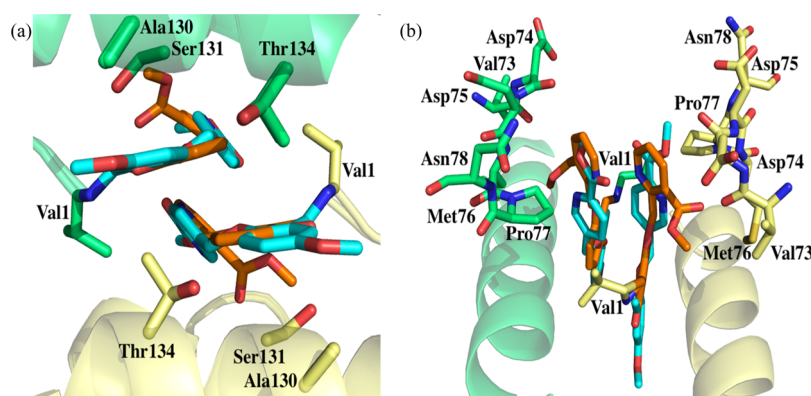


Figure 11. Structural comparison of compounds **6** and **9** bound at the α -cleft of Hb. (a) superposition of compounds **6** and **9** molecules showing interactions with residues from α F-helix. (b) 90° rotated view of (a). (Hb is shown as cartoon with $\alpha 1$ subunit in green and $\alpha 2$ in yellow; compounds **6** and **9** are shown in cyan and orange sticks, respectively).

with $\alpha 2$ Val73, $\alpha 2$ Asp74, and $\alpha 2$ Pro77 (2.7–4.0 Å) residues, which in TD-7 is relatively weaker (3.5–4.3 Å).³⁵ These α F-helix interactions, we believe lead to perturbation of the helix to destabilize the polymer, explaining the unusually high antisickling effect (through O_2 -independent mechanism) at the relatively low P_{50} shift of this compound. As noted above, GBT-440 also binds to the α -cleft of the R2-state Hb to make Schiff-base interaction with the α Val1 amine. Interestingly, unlike our compounds and previously studied aromatic aldehydes that bind two molecules, one each to $\alpha 1$ -subunit and $\alpha 2$ -subunit, GBT-440 only binds one molecule at the α -cleft because of the isopropyl–pyrazole substituent that sterically prevents two molecules from binding.⁵² Nonetheless, unlike compound **9**, GBT-440 does not make any close contact with the α F-helix, and thus, we do not expect this molecule to have any significant O_2 -independent antisickling activity, consistent with our comparative study that show strong correlation between its P_{50} shift and antisickling activity, and also as reported in the literature.⁵²

Similar to compound **9**, compound **6** also binds with the pyridylmethoxy-methyl ester group orientated toward the α F-helix. Nonetheless, the ester group forms stronger intrasubunit hydrophobic interactions with $\alpha 2$ Pro77 (3.1 c5) compared to compound **9** (3.5 c5) (Figures 10 and 11). In addition, the methoxy groups of the ester form several water-mediated hydrogen bonding interactions with the backbone atoms of $\alpha 2$ Val73, $\alpha 2$ Asp75, and $\alpha 2$ Met76 of the α F-helix (Figure 10). Similar to compound **9**, compound **6** interactions with the α F-helix likely lead to perturbation of the α F-helix, consistent with this compound unusually potent antisickling effect when compared to the relatively small effect on the Hb oxygen affinity.

Compounds Showed Improved *In Vivo* PD Effects.

Through systematic SAR studies, we successfully identified several compounds that showed significantly enhanced pharmacologic activity *in vitro* compared to the previous precursor TD-7. Several of these compounds showed sustained action over 24 h. Among the most potent compounds identified, compounds **9** and **10** were selected for further *in vivo* PD studies using wild-type mice (C57BL/6). The mice received a single IP dose of 150 mg/kg (a total of 6 mice). Blood samples were obtained prior to treatment (0), and 1, 3, and 6 h post treatment, via submandibular bleeding and subjected to hemolysis using standard methods. Clarified lysates, free of cell debris and RBC ghosts, were analyzed by

cation-exchange HPLC to determine the levels of drug-modified Hb (adducts) and to conduct OEC studies to determine the degree of P_{50} shift or Hb- O_2 affinity.

All compounds showed significant *in vivo* modification of intracellular Hb with increasing levels from 1 h to the 6 h experimental period (Figure 12). Mice treated with compound

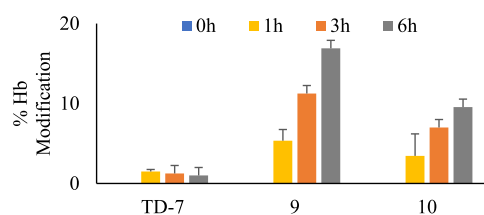


Figure 12. Time-dependent modification of Hb in wild-type mice ($n = 6$) after 150 mg/kg IP administration of test compounds.

9 demonstrated the highest levels of modified Hb ($16.9 \pm 1.0\%$ at 6 h), followed by compound **10** ($9.6 \pm 1.9\%$). Only $1.5 \pm 0.3\%$ modified Hb was observed in mice treated with the control TD-7. Corresponding changes were observed in oxygen affinity at the measured time points of 3 and 6 h (Figure 13). Mice treated with compound **9** showed the

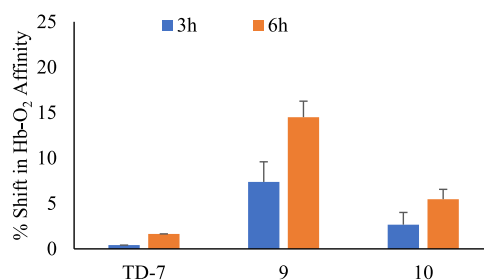


Figure 13. Time-dependent Hb- O_2 affinity shifts in the wild-type mice ($n = 6$) after 150 mg/kg IP administration of test compounds.

highest levels of shifts ($14.5\% \pm 2.2$ at 6 h). Compound **10** also increased Hb- O_2 affinity, although relatively lower by $5.5\% \pm 1.9$. In contrast, only approximately $1\% \pm 0.2$ shift in the Hb- O_2 affinity was observed in the mice treated with TD-7. These preliminary *in vivo* studies demonstrate improvement in the pharmacologic profile of our aromatic aldehyde class of allosteric effectors of Hb.

CONCLUSIONS

Intracellular polymerization of deoxygenated sickle hemoglobin remains the principal cause of the pathophysiology associated with SCD. Naturally occurring and synthetic AEHs have been investigated as potential therapeutic agents for the treatment of SCD.^{33,35,36,39–41,52} Even though this class of compounds showed significant potency *in vitro*, several of them lack good PK properties and therefore are not feasible to treat a chronic disease that requires significant levels of Hb modification for efficacy. These drawbacks have severely hampered the clinical development and utility of aromatic aldehydes to treat SCD. For example, our group studied 5-HMF; however, because of metabolic instability of the aldehyde that translated to poor oral bioavailability, the phase II clinical study was terminated.^{24,56} In previous reports, our group has demonstrated a systematic and rational structure-based approach to develop several aromatic aldehydes that exhibited excellent antisickling activity. In the current report, we modified the TD compounds to overcome the disadvantages associated with potency and oxidative metabolism by derivatizing the methyl alcohol on the pyridines to a methyl ester as well as protecting the aromatic aldehyde with an *ortho*-hydroxy group. These compounds exhibited several novel properties that are missing from the previous generation compounds. They showed sustained pharmacologic activity *in vitro*, as well as both sustained and significantly improved activity *in vivo*. Remarkably, some of the compounds potentially exhibited additional mechanism of action independent of the primary O₂-dependent antisickling effect. Structural studies of compounds **6** and **9** complexes provided plausible explanations for these enhanced antisickling activities that involves perturbing the α F-helix leading to O₂-independent antisickling activity. These novel results are encouraging and provide guidance for the further development of potent antisickling lead compounds. Compounds **9**, **10**, and **13** are currently undergoing formulation for detailed *in vivo* PD studies.

EXPERIMENTAL SECTION

Chemistry. All reagents used in the synthesis and functional assays were purchased from Sigma-Aldrich (St. Louis, MO) or Thermo Fisher Scientific (Waltham, MA) and utilized without additional purification. ¹H NMR and ¹³C NMR spectra were obtained on a Bruker 400 MHz spectrometer, and tetramethylsilane was used as an internal standard. Peak positions are given in parts per million (δ). Column chromatography was performed on silica gel (grade 60 mesh; Bodman Industries, Aston, PA). Routine thin-layer chromatography was performed on silica gel GHIF plates (250 μ m, 2.5 \times 10 cm; Analtech Inc., Newark, DE). MS spectra were obtained from a PerkinElmer Flexar UHPLC with an AxION 2 time-of-flight mass spectrometer, and the molecular weight of the compounds was within 0.005% of calculated values. Infrared spectra were obtained on Thermo Nicolet iS10 FT-IR. Purity of the compounds was determined by HPLC using Varian Microsorb 100-5 C18 column (250 \times 4.6 mm), using Prostar 325 UV-vis (210 nm) as the detector. The HPLC parameters used were injection volume = 15 μ L, sample concentration = 3 mM, mobile phase = 60MeCN–40H₂O, flow rate = 1 mL/min.

The compounds were synthesized according to the general procedures for similar compounds.^{33,35,39}

General Procedure for the Synthesis of Compounds i–vii. A mixture of the methyl-substituted pyridylmethyl ester (1 equiv) and α,α' -azoisobutyronitrile (AIBN) (10%) was dissolved in carbon tetrachloride (CCl₄). The solution was heated at 48 °C, and NBS (1.1 equiv) solution in CCl₄ was added dropwise and stirred for 5 h. The

reaction was cooled to room temperature, and the solvent evaporated. The mixture was then extracted using dichloromethane and water followed by washing the organic layer with brine. The organic layer was dried over sodium sulfate, filtered, evaporated, and the crude product was purified using column chromatography.

Methyl 5-(bromomethyl)nicotinate (**vi**) and methyl 2-(bromomethyl)benzoate (**vii**) were purchased from Sigma-Aldrich (St. Louis, MO).

Methyl 6-(Bromomethyl)nicotinate (i).⁵⁷ The title compound was prepared following the general procedure as a white solid in 66% yield. ¹H NMR (400 MHz, DMSO-*d*₆): δ 9.16 (d, *J* = 1.56 Hz, 1H), 8.30 (dd, *J* = 8.12, 2.2 Hz, 1H), 7.53 (dd, *J* = 8.12, 0.48 Hz, 1H), 4.58 (s, 2H), 3.96 (s, 3H). MS (ESI) *m/z*: 229.98 [M + H]⁺.

Methyl 2-(Bromomethyl)nicotinate (ii).⁵⁸ The title compound was prepared following the general procedure as an orange solid in 65% yield. ¹H NMR (400 MHz, DMSO-*d*₆): δ 8.71 (dd, *J* = 4.8, 1.76 Hz, 1H), 8.28 (dd, *J* = 7.92, 1.76 Hz, 1H), 7.33 (m, 1H), 5.04 (s, 2H), 3.98 (s, 3H). MS (ESI) *m/z*: 229.98 [M + H]⁺.

Methyl 6-(Bromomethyl)picolinate (iii).⁵⁹ The title compound was prepared following the general procedure as a white solid in 66% yield. ¹H NMR (400 MHz, DMSO-*d*₆): δ 8.05 (d, *J* = 7.68 Hz, 1H), 7.99 (t, *J* = 7.72 Hz, 1H), 7.77 (d, *J* = 7.68 Hz, 1H), 4.67 (s, 2H), 3.98 (s, 3H). MS (ESI) *m/z*: 229.98 [M + H]⁺.

Methyl 2-(Bromomethyl)isonicotinate (iv).⁶⁰ The title compound was prepared following the general procedure as a dark blue solid in 66% yield. ¹H NMR (400 MHz, DMSO-*d*₆): δ 8.77 (dd, *J* = 5, 0.64 Hz, 1H), 8.02 (m, 1H), 7.77 (dd, *J* = 5, 1.56 Hz, 1H), 4.81 (s, 2H), 3.91 (s, 3H). MS (ESI) *m/z*: 229.98 [M + H]⁺.

Methyl 5-(Bromomethyl)picolinate (v).⁶¹ The title compound was prepared following the general procedure as a white solid in 66% yield. ¹H NMR (400 MHz, DMSO-*d*₆): δ 8.78 (t, *J* = 1.48 Hz, 1H), 8.06 (d, *J* = 1.36 Hz, 2H), 4.82 (s, 2H), 3.89 (s, 3H). MS (ESI) *m/z*: 229.98 [M + H]⁺.

General Procedure for Synthesis of Compounds 1–14. A mixture of 2-hydroxy-5-methoxybenzaldehyde or 2,6-dihydroxybenzaldehyde (1 equiv) and corresponding bromo-pyridinylmethoxy-methyl ester (1 equiv) was dissolved in anhydrous *N,N*-dimethylformamide (DMF). Anhydrous potassium carbonate (K₂CO₃) (1.2 equiv) was added to this mixture, and the reaction was stirred at room temperature for 8–10 h. The solvent was then evaporated, and the reaction mixture extracted with ethyl acetate and water. The organic layer was dried over sodium sulfate, filtered, solvent evaporated, and the crude product was purified using column chromatography.

Methyl 6-((2-Formyl-4-methoxyphenoxy)methyl)nicotinate (1). The title compound was prepared following the general procedure as a white solid in 82% yield. IR (Diamond, cm⁻¹): 2922, 2867, 1721, 1669, 1620, 1585, 1499, 1446, 1391, 1370, 1286, 1224, 1174, 1141, 1121; ¹H NMR (400 MHz, DMSO-*d*₆): δ 10.49 (s, 1H), 9.08 (m, 1H), 8.36 (dd, *J* = 8.16, 2.16 Hz, 1H), 7.80 (d, *J* = 8.12 Hz, 1H), 7.25 (m, 3H), 5.42 (s, 2H), 3.91 (s, 3H), 3.77 (s, 3H); ¹³C NMR (100 MHz, DMSO-*d*₆): δ 188.94, 165.00, 161.04, 154.62, 153.62, 149.59, 137.82, 125.03, 124.77, 122.85, 121.31, 115.97, 110.78, 71.02, 55.59, 52.38. Mass spectrum *m/z*: found 324.07 [M + Na]⁺; calcd, 324.08 [M + Na]⁺. The purity of the compound was checked by HPLC and was found to be 96% pure.

Methyl 2-((2-Formyl-4-methoxyphenoxy)methyl)nicotinate (2). The title compound was prepared following the general procedure as a pale yellow solid in 82% yield. IR (Diamond, cm⁻¹): 2920, 1719, 1684, 1667, 1622, 1583, 1535, 1492, 1445, 1404, 1372, 1276, 1215, 1168, 1142; ¹H NMR (400 MHz, DMSO-*d*₆): δ 10.25 (s, 1H), 8.74 (dd, *J* = 4.76, 1.48 Hz, 1H), 8.23 (dd, *J* = 7.8, 1.44 Hz, 1H), 7.55 (m, 1H), 7.2 (m, 3H), 5.56 (s, 2H), 3.78 (s, 3H), 3.75 (s, 3H); ¹³C NMR (100 MHz, DMSO-*d*₆): δ 188.73, 166.14, 155.39, 155.29, 153.46, 151.55, 138.47, 126.17, 124.86, 123.66, 122.98, 116.13, 110.06, 70.98, 55.61, 52.54. Mass spectrum *m/z*: found 302.11 [M + H]⁺, 324.09 [M + Na]⁺; calcd, 302.10 [M + H]⁺, 324.08 [M + Na]⁺. The purity of the compound was checked by HPLC and was found to be 98% pure.

Methyl 6-((2-Formyl-4-methoxyphenoxy)methyl)picolinate (3). The title compound was prepared following the general procedure as

a white solid in 82% yield. IR (Diamond, cm^{-1}): 2953, 2851, 1720, 1682, 1618, 1585, 1494, 1396, 1369, 1296, 1222, 1169, 1141; ^1H NMR (400 MHz, $\text{DMSO}-d_6$): δ 10.47 (s, 1H), 8.03 (m, 2H), 7.87 (d, $J = 7.32$ Hz, 1H), 7.26 (m, 3H), 5.38 (s, 2H), 3.90 (s, 3H), 3.76 (s, 3H); ^{13}C NMR (100 MHz, $\text{DMSO}-d_6$): δ 189.03, 164.99, 156.95, 154.68, 153.59, 146.99, 138.57, 125.05, 125.01, 123.95, 123.84, 115.99, 110.76, 71.08, 55.59, 52.39. Mass spectrum m/z : found 302.10 $[\text{M} + \text{H}]^+$, 324.08 $[\text{M} + \text{Na}]^+$; calcd, 302.10 $[\text{M} + \text{H}]^+$, 324.08 $[\text{M} + \text{Na}]^+$. The purity of the compound was checked by HPLC and was found to be 98% pure.

Methyl 2-((2-Formyl-4-methoxyphenoxy)methyl)isonicotinate (4). The title compound was prepared following the general procedure as a white solid in 82% yield. IR (Diamond, cm^{-1}): 2923, 1729, 1686, 1608, 1566, 1450, 1382, 1292, 1276, 1216, 1190, 1171; ^1H NMR (400 MHz, $\text{DMSO}-d_6$): δ 10.43 (s, 1H), 8.81 (dd, $J = 5, 0.56$ Hz, 1H), 8.02 (s, $J = 1.44$ Hz, 1H), 7.80 (dd, $J = 5.04, 1.56$ Hz, 1H), 7.24 (m, 3H), 5.41 (s, 2H), 3.91 (s, 3H), 3.76 (s, 3H); ^{13}C NMR (100 MHz, $\text{DMSO}-d_6$): δ 188.81, 165.02, 157.80, 154.78, 153.63, 150.44, 137.79, 125.09, 122.92, 121.82, 120.33, 116.25, 110.73, 71.27, 55.58, 52.81. Mass spectrum m/z : found 302.10 $[\text{M} + \text{H}]^+$, 324.08 $[\text{M} + \text{Na}]^+$; calcd, 302.10 $[\text{M} + \text{H}]^+$, 324.08 $[\text{M} + \text{Na}]^+$. The purity of the compound was checked by HPLC and was found to be 98% pure.

Methyl 3-((2-Formyl-4-methoxyphenoxy)methyl)picolininate (5). The title compound was prepared following the general procedure as a pale yellow solid in 80% yield. IR (Diamond, cm^{-1}): 2897, 1712, 1671, 1607, 1567, 1490, 1445, 1398, 1365, 1275, 1232, 1165, 1139, 1106; ^1H NMR (400 MHz, $\text{DMSO}-d_6$): δ 10.35 (s, 1H), 8.65 (dd, $J = 4.6, 1.28$ Hz, 1H), 8.2 (dd, $J = 7.84, 0.76$ Hz, 1H), 7.66 (dd, $J = 7.88, 4.68$ Hz, 1H), 7.24 (m, 3H), 5.49 (s, 2H), 3.83 (s, 3H), 3.77 (s, 3H); ^{13}C NMR (100 MHz, $\text{DMSO}-d_6$): δ 188.81, 166.12, 154.66, 153.55, 148.49, 146.69, 136.89, 133.04, 126.43, 124.89, 122.96, 115.79, 110.68, 67.44, 55.56, 52.34. Mass spectrum m/z : found 324.08 $[\text{M} + \text{Na}]^+$; calcd, 324.08 $[\text{M} + \text{Na}]^+$. The purity of the compound was checked by HPLC and was found to be 98% pure.

Methyl 5-((2-Formyl-4-methoxyphenoxy)methyl)picolininate (6). The title compound was prepared following the general procedure as a pale yellow solid in 80% yield. IR (Diamond, cm^{-1}): 2962, 2864, 2767, 1719, 1684, 1673, 1588, 1489, 1458, 1395, 1355, 1274, 1218, 1198, 1150, 1127; ^1H NMR (400 MHz, $\text{DMSO}-d_6$): δ 10.40 (s, 1H), 8.84 (d, $J = 1.36$ Hz, 1H), 8.10 (m, 2H), 7.28 (m, 2H), 7.2 (d, $J = 2.92$ Hz, 1H), 5.39 (s, 2H), 3.89 (s, 3H), 3.76 (s, 3H); ^{13}C NMR (100 MHz, $\text{DMSO}-d_6$): δ 188.77, 154.89, 154.57, 148.62, 135.93, 135.67, 135.93, 135.67, 125.92, 125.17, 123.28, 114.92, 111.30, 68.52, 55.90, 52.97. Mass spectrum m/z : found 302.10 $[\text{M} + \text{H}]^+$, 324.09 $[\text{M} + \text{Na}]^+$; calcd, 302.10 $[\text{M} + \text{H}]^+$, 324.08 $[\text{M} + \text{Na}]^+$. The purity of the compound was checked by HPLC and was found to be 98% pure.

Methyl 5-((2-Formyl-4-methoxyphenoxy)methyl)nicotinate (7). The title compound was prepared following the general procedure as a white solid in 82% yield. IR (Diamond, cm^{-1}): 2969, 1718, 1670, 1602, 1572, 1498, 1435, 1405, 1382, 1279, 1217, 1185, 1160, 1119; ^1H NMR (400 MHz, $\text{DMSO}-d_6$): δ 10.37 (s, 1H), 9.06 (d, $J = 2$ Hz, 1H), 8.97 (d, $J = 2.04$ Hz, 1H), 8.42 (t, $J = 2.04$ Hz, 1H), 7.29 (m, 2H), 7.2 (d, $J = 3.08$ Hz, 1H), 5.38 (s, 2H), 3.9 (s, 3H), 3.77 (s, 3H); ^{13}C NMR (100 MHz, $\text{DMSO}-d_6$): δ 188.87, 165.04, 154.64, 153.64, 152.90, 149.49, 135.99, 132.63, 125.44, 125.13, 122.88, 116.21, 110.71, 67.83, 55.58, 52.49. Mass spectrum m/z : found 324.08 $[\text{M} + \text{Na}]^+$; calcd, 324.08 $[\text{M} + \text{Na}]^+$. The purity of the compound was checked by HPLC and was found to be 99% pure.

Methyl 6-((2-Formyl-3-hydroxyphenoxy)methyl)nicotinate (8). The title compound was prepared following the general procedure as a white solid in 58% yield. IR (Diamond, cm^{-1}): 3299, 2959, 1726, 1694, 1620, 1458, 1437, 1382, 1343, 1285, 1233, 1172, 1122; ^1H NMR (400 MHz, $\text{DMSO}-d_6$): δ 11.73 (s, 1H), 10.45 (s, 1H), 9.09 (s, 1H), 8.34 (d, $J = 8.12$ Hz, 1H), 7.81 (d, $J = 8.28$ Hz, 1H), 7.51 (t, $J = 8.4$ Hz, 1H), 6.67 (d, $J = 8.52$ Hz, 1H), 6.56 (d, $J = 8.36$ Hz) 5.41 (s, 2H), 3.90 (s, 3H); ^{13}C NMR (100 MHz, $\text{DMSO}-d_6$): δ 193.85, 165.39, 163.86, 160.84, 160.41, 150.66, 138.40, 138.12, 125.47, 120.52, 111.05, 110.86, 102.24, 70.91, 52.47. Mass spectrum m/z : found 288.08 $[\text{M} + \text{H}]^+$, 310.08 $[\text{M} + \text{Na}]^+$; calcd, 288.08 $[\text{M} + \text{H}]^+$,

309.06 $[\text{M} + \text{Na}]^+$. The purity of the compound was checked by HPLC and was found to be 99% pure.

Methyl 2-((2-Formyl-3-hydroxyphenoxy)methyl)nicotinate (9). The title compound was prepared following the general procedure as a pale yellow solid in 58% yield. IR (Diamond, cm^{-1}): 2956, 1713, 1618, 1637, 1571, 1459, 1435, 1396, 1370, 1287, 1238, 1170, 1141; ^1H NMR (400 MHz, $\text{DMSO}-d_6$): δ 11.67 (s, 1H), 10.19 (s, 1H), 8.75 (dd, $J = 4.8, 1.68$ Hz, 1H), 8.25 (dd, $J = 7.84, 1.68$ Hz, 1H), 7.55 (m, 2H), 6.66 (d, $J = 8.2$ Hz, 1H), 6.53 (d, $J = 8.4$ Hz, 1H), 5.58 (s, 2H), 3.79 (s, 3H); ^{13}C NMR (100 MHz, $\text{DMSO}-d_6$): δ 193.68, 166.15, 162.26, 161.44, 155.02, 151.73, 138.75, 138.31, 126.02, 123.60, 110.66, 109.49, 103.51, 70.59, 52.50. Mass spectrum m/z : found 288.09 $[\text{M} + \text{H}]^+$, 310.07 $[\text{M} + \text{Na}]^+$; calcd, 288.08 $[\text{M} + \text{H}]^+$, 309.06 $[\text{M} + \text{Na}]^+$. The purity of the compound was checked by HPLC and was found to be 99% pure.

Methyl 6-((2-Formyl-3-hydroxyphenoxy)methyl)picolininate (10). The title compound was prepared following the general procedure as a pale yellow solid in 60% yield. IR (Diamond, cm^{-1}): 3065, 3010, 2956, 2890, 1738, 1697, 1640, 1614, 1583, 1462, 1454, 1400, 1358, 1297, 1242, 1190, 1171, 1150; ^1H NMR (400 MHz, $\text{DMSO}-d_6$): δ 11.74 (s, 1H), 10.44 (s, 1H), 8.04 (m, 2H), 7.91 (dd, $J = 7.48, 1.12$ Hz, 1H), 7.52 (t, $J = 8.4$ Hz, 1H), 6.7 (d, $J = 8$ Hz, 1H), 6.56 (d, $J = 8.4$ Hz, 1H), 5.39 (s, 2H), 3.90 (s, 3H); ^{13}C NMR (100 MHz, $\text{DMSO}-d_6$): δ 193.79, 164.99, 162.43, 160.69, 160.62, 149.59, 138.65, 137.84, 124.81, 121.26, 110.79, 109.81, 103.42, 70.49, 52.41. Mass spectrum m/z : found 288.09 $[\text{M} + \text{H}]^+$, 310.07 $[\text{M} + \text{Na}]^+$; calcd, 288.08 $[\text{M} + \text{H}]^+$, 309.06 $[\text{M} + \text{Na}]^+$. The purity of the compound was checked by HPLC and was found to be 99% pure.

Methyl 2-((2-Formyl-3-hydroxyphenoxy)methyl)isonicotinate (11). The title compound was prepared following the general procedure as a pale yellow solid in 58% yield. IR (Diamond, cm^{-1}): 2961, 1733, 1716, 1639, 1620, 1577, 1460, 1441, 1373, 1342, 1293, 1235, 1215, 1174; ^1H NMR (400 MHz, $\text{DMSO}-d_6$): δ 11.68 (s, 1H), 10.39 (s, 1H), 8.81 (dd, $J = 5, 0.6$ Hz, 1H), 8.03 (d, $J = 0.56$ Hz, 1H), 7.81 (dd, $J = 5, 1.56$ Hz, 1H), 7.51 (t, $J = 8.4$ Hz, 1H), 5.41 (s, 2H), 3.91 (s, 3H); ^{13}C NMR (100 MHz, $\text{DMSO}-d_6$): δ 193.51, 165.02, 162.37, 160.80, 157.43, 150.43, 138.66, 137.84, 121.89, 120.38, 110.83, 109.74, 103.56, 70.69, 52.83. Mass spectrum m/z : found 288.09 $[\text{M} + \text{H}]^+$, 310.07 $[\text{M} + \text{Na}]^+$; calcd, 288.08 $[\text{M} + \text{H}]^+$, 309.06 $[\text{M} + \text{Na}]^+$. The purity of the compound was checked by HPLC and was found to be 99% pure.

Methyl 3-((2-Formyl-3-hydroxyphenoxy)methyl)picolininate (12). The title compound was prepared following the general procedure as a pale yellow solid in 54% yield. IR (Diamond, cm^{-1}): 3092, 2923, 2851, 1774, 1712, 1632, 1599, 1566, 1515, 1478, 1366, 1276, 1231, 1180, 1136, 1072; ^1H NMR (400 MHz, $\text{DMSO}-d_6$): δ 11.72 (s, 1H), 10.32 (s, 1H), 8.65 (dd, $J = 4.64, 1.52$ Hz, 1H), 8.22 (m, 1H), 7.66 (dd, $J = 7.88, 4.64$ Hz, 1H), 7.54 (t, $J = 8.4$ Hz, 1H), 6.66 (d, $J = 8$ Hz, 1H), 6.57 (d, $J = 8.4$ Hz, 1H), 5.51 (s, 2H), 3.84 (s, 3H); ^{13}C NMR (100 MHz, $\text{DMSO}-d_6$): δ 193.59, 166.09, 162.46, 160.68, 148.53, 146.54, 138.72, 136.83, 132.78, 126.44, 110.74, 109.79, 103.26, 67.04, 52.35. Mass spectrum m/z : found 310.08 $[\text{M} + \text{Na}]^+$; calcd, 309.06 $[\text{M} + \text{Na}]^+$. The purity of the compound was checked by HPLC and was found to be 99% pure.

Methyl 5-((2-Formyl-3-hydroxyphenoxy)methyl)picolininate (13). The title compound was prepared following the general procedure as a white solid in 54% yield. IR (Diamond, cm^{-1}): 2954, 1731, 1679, 1644, 1618, 1574, 1458, 1440, 1392, 1357, 1289, 1249, 1177, 1144, 1122; ^1H NMR (400 MHz, $\text{DMSO}-d_6$): δ 11.74 (s, 1H), 10.37 (s, 1H), 8.86 (s, 1H), 8.12 (m, 2H), 7.54 (t, $J = 8.4$ Hz, 1H), 6.72 (d, $J = 8.32$ Hz, 1H), 6.56 (d, $J = 8.4$ Hz, 1H), 5.40 (s, 2H), 3.89 (s, 3H); ^{13}C NMR (100 MHz, $\text{DMSO}-d_6$): δ 193.83, 162.42, 160.69, 148.72, 147.01, 138.64, 136.32, 135.91, 135.78, 124.64, 109.79, 103.37, 67.31, 52.39. Mass spectrum m/z : found 310.08 $[\text{M} + \text{Na}]^+$; calcd, 310.08 $[\text{M} + \text{Na}]^+$. The purity of the compound was checked by HPLC and was found to be 99% pure.

Methyl 5-((2-Formyl-3-hydroxyphenoxy)methyl)nicotinate (14). The title compound was prepared following the general procedure as a white solid in 54% yield. IR (Diamond, cm^{-1}): 2907, 1719, 1643, 1617, 1584, 1460, 1429, 1397, 1370, 1292, 1246, 1179, 1152, 1121; ^1H

NMR (400 MHz, DMSO- d_6): δ 11.72 (s, 1H), 10.33 (s, 1H), 9.05 (d, $J = 1.8$ Hz, 1H), 8.99 (d, $J = 1.76$ Hz, 1H), 8.43 (t, $J = 2$ Hz, 1H), 7.55 (t, $J = 8.2$ Hz, 1H), 6.73 (d, $J = 8.2$ Hz, 1H), 6.56 (d, $J = 8.44$ Hz, 1H), 5.39 (s, 2H), 3.91 (s, 3H); ^{13}C NMR (100 MHz, DMSO- d_6): δ 193.74, 176.82, 165.04, 162.40, 160.72, 152.87, 149.53, 138.63, 135.99, 132.32, 110.80, 109.76, 103.42, 67.28, 52.49. Mass spectrum m/z : found 288.08 $[\text{M} + \text{H}]^+$; calcd, 288.08 $[\text{M} + \text{H}]^+$. The purity of the compound was checked by HPLC and was found to be 99% pure.

Blood. Normal whole blood was collected from adult donors at the Virginia Commonwealth University after informed consent, in accordance with regulations of the IRB for Protection of Human Subjects. Hb was purified from discarded normal blood samples using standard procedures.⁶² Leftover blood samples from individuals with homozygous SS were obtained and utilized, based on an approved IRB protocol at the Children's Hospital of Philadelphia, with informed consent.

Oxygen Equilibrium Curve Studies. The OEC study to determine the effect of the compounds on Hb affinity for oxygen was conducted following the standard procedure.^{34,41} Whole blood (30% hematocrit) was incubated in the absence or presence of compounds (0.5, 1.0, and 2.0 mM) solubilized in DMSO. Following, the blood-compound samples were incubated in an IL 237 tonometer (Instrumentation Laboratories, Inc., Lexington, MA) for about 7 min at 37 °C against a gas mixture containing O_2 concentrations of 0.804, 2.935, and 5.528% and allowed to equilibrate at O_2 tensions of 6, 20, and 40 mmHg. After equilibration, the sample was removed via syringe and aspirated into a ABL 700 series table top automated blood gas analyzer (Radiometer America, Inc., Westlake, OH) to determine total hemoglobin (tHb), hematocrit (H_{ct}), pH, $p\text{CO}_2$, partial pressure of oxygen ($p\text{O}_2$), and the Hb- O_2 saturation ($s\text{O}_2$) values. The measured values of $p\text{O}_2$ and $s\text{O}_2$ at each oxygen saturation level were then subjected to nonlinear regression analysis using the software Scientist (Micromath, Salt Lake City UT) with the following equation

$$s\text{O}_2\% = 100 \times \frac{p\text{O}_2^N \text{ mmHg}}{P_{50}^N (\text{mmHg}) + p\text{O}_2^N (\text{mmHg})}$$

This equation was used to calculate P_{50} and Hill coefficient (N) values. ΔP_{50} (%) was determined as

$$\Delta P_{50}(\%) = 100 \times \left(\frac{P_{50} \text{ in the absence of compound} - P_{50} \text{ in the presence of compound}}{P_{50} \text{ in the absence of compound}} \right)$$

For concentration-dependent OEC studies, 0.5, 1.0, and 2 mM concentrations of each compound to be tested were used, whereas for time-dependent OEC studies, 2 mM of each compound was used. Aliquots of each sample was tested at 1, 2, 4, 8, 12, and 24 h to obtain the P_{50} and ΔP_{50} values.

Hemoglobin Modification, Oxygen Equilibrium, and Anti-sickling Studies Using Human Sickle Blood. Blood suspensions from subjects with homozygous SCD (hematocrit 20%) were incubated under air in the absence or presence of compounds (0.5, 1, and 2 mM) at 37 °C for 1 h to ensure that binding has attained equilibrium. Following, the suspensions were incubated under hypoxic conditions (certified gas mix of 2.5% O_2 /97.5% N_2) at 37 °C for 2 h. Aliquot samples were fixed with 2% glutaraldehyde solution without exposure to air and then subjected to microscopic morphological analysis of bright field images (at 40X magnification) of single layer cells on an Olympus BX40 microscope fitted with an Infinity 2 camera (Olympus) and the coupled Image Capture software. The residual samples were washed in phosphate-buffer saline and hemolyzed in hypotonic lysis buffer for subsequent analyses.^{38,41}

For oxygen equilibrium studies, approximately, 100 μL aliquot samples from the above-clarified lysate were added to 4 mL of 0.1 M potassium phosphate buffer, pH 7.0, in cuvettes and subjected to hemoximetry analysis using the Hemox Analyzer (TCS Scientific Corp., New Hope, PA) to assess P_{50} shifts. Degree of Hb- O_2 affinity shift (ΔP_{50}) was expressed as percentage fractions of control DMSO-treated samples.

Finally, for the Hb adduct formation studies, the above-clarified lysates were subjected to cation-exchange HPLC (Hitachi D-7000 Series, Hitachi Instruments, Inc., San Jose, CA), using a weak cation-exchange column (Poly CAT A: 30 mm \times 4.6 mm, Poly LC, Inc., Columbia, MD). A commercial standard consisting of approximately equal amounts of composite HbF, HbA, HbS, and HbC (Helena Laboratories, Beaumont, TX) was utilized as reference isotopes. The areas of new peaks, representing HbS adducts, were obtained, calculated as percentage fractions of total Hb area and reported as levels of modified Hb.

Stability Studies of Compounds Using Whole Blood. Normal whole blood (hematocrit 30%) was incubated in the absence and presence of 0.5 and 1 mM of compounds **9** and **10**. Aliquots were removed at 0, 4, 8, and 24 h of incubation, and deproteinization was carried out using 0.1 M formic acid in acetonitrile (HPLC grade) at 60–65 °C for 30 min. Following this, the samples were centrifuged at 12,000 rpm for 20 min to obtain a clear supernatant which was sequentially filtered through 0.43 and 0.22 μm filters to further clean the samples for HPLC analysis. Compounds **9**, **10**, and the corresponding carboxylic acid derivative of compound **10** were used as the positive controls, while blood in the absence of any compound was used as the negative control. HPLC analysis was carried out at 261 nm wavelength using the Phenomenex Luna C18 5 μ 100A 150 \times 4.6 mm column with a gradient consisting 0.1% formic acid in water (Buffer A) and 0.1% formic acid in acetonitrile (Buffer B) and a flow rate of 1.5 mL/min. Elution times for compounds and their metabolites were approximately 9.6 and 11.8 min, respectively.

X-ray Crystallography. Co-crystals of liganded Hb with compounds **6** and **9** were obtained following similar reported procedures.^{35,39} In short, freshly made solution of compound in DMSO was added to deoxygenated (deoxy) Hb (30 mg/mL protein) at an Hb tetramer-compound ratio of 1:10. Following, the complex mixture was saturated with carbon monoxide and allowed to incubate for 2 h to form the COHb-compound complex. Sodium cyanoborohydride (NaBH_3CN) was then added to this mixture to reduce the Schiff-base adduct formed between the protein and compound to the corresponding irreversible alkylamine covalent bond. The resulting solution was crystallized using 10–20% PEG6000, 100 mM HEPES buffer, and pH 7.4 using the batch method as previously published. Single-cherry red needle crystals were formed in 1–3 days and were used to collect X-ray diffraction data at 100 K using Rigaku MicroMax 007HF X-ray Generator, Eiger R 4M Detector, and Oxford Cobra Cryo-system (The Woodlands, TX). The crystals were first cryoprotected with 80 μL mother liquor mixed with 62 μL of 50% PEG6000. The data set was processed with the CrysAlis PRO 2015 program (Rigaku Oxford Diffraction Ltd. Yarnton, Oxfordshire, England) and the CCP4 suite of programs.⁶³ The crystal structures of the COHb-compound complexes were determined by a molecular replacement method with the Phenix program,^{53,64} using the native R2-state crystal structure (PDB ID 1BBB) as a search model. The structures were refined using both Phenix and CNS, while model building and correction were carried out using COOT.^{54,55}

In Vivo Pharmacologic Effect of Compounds in Wild-Type Mice. We tested *in vivo* pharmacologic effects of compounds **9** and **10** (and TD-7 as control) in C57BL/6 mice. All animal experiments were performed according to the institutional ethical guidelines on animal care and approved by the Institute Animal Care and Use Committee at the Children's Hospital of Philadelphia (approval number: IAC 19-000113). Equal numbers of male ($n = 3$) and female ($n = 3$) mice were used for the study. The animals were treated with a single intraperitoneal (IP) (150 mg/kg) dose of the compounds. Blood samples were obtained prior to treatment (0) and 1, 3, and 6 h post-treatment, via submandibular bleeding, and subjected to hemolysis using standard methods. Clarified lysates, free of cell debris, and RBC ghosts were analyzed by cation-exchange HPLC to determine the levels of drug-modified hemoglobin (adducts) and utilized to conduct oxygen equilibrium studies to determine degrees of shift in P_{50} values using methodologies described earlier for *in vitro* studies on human samples.

Statistical Analyses. All functional and biological assays evaluating antisickling properties, Hb modification, and oxygen affinity changes were conducted in three biological replicates. Results are reported as mean values with standard deviations, from triplicate analyses.

■ ASSOCIATED CONTENT

SI Supporting Information

The Supporting Information is available free of charge at <https://pubs.acs.org/doi/10.1021/acs.jmedchem.0c01287>.

Molecular formula strings (CSV)

OEC of final compounds; final $2F_o - F_c$ electron density map of COHb-6 and COHb-9 complexes; representative plot for cation-exchange HPLC patterns of modified Hb; spectral data of final compounds (^1H and ^{13}C graphs); and purity data of final compounds (HPLC graphs) (PDF)

Accession Codes

The atomic coordinate and structure factor files have been submitted to the Protein Data Bank under accession codes 6XDT and 6XE7 for the complex structures of compounds 6 and 9, respectively. Authors will release the atomic coordinates and experimental data upon article publication.

■ AUTHOR INFORMATION

Corresponding Authors

Yan Zhang – Department of Medicinal Chemistry and The Institute for Structural Biology, Drug Discovery, and Development, School of Pharmacy, Virginia Commonwealth University, Richmond, Virginia 23298, United States; orcid.org/0000-0001-8934-7016; Email: yzhang2@vcu.edu

Martin K. Safo – Department of Medicinal Chemistry and The Institute for Structural Biology, Drug Discovery, and Development, School of Pharmacy, Virginia Commonwealth University, Richmond, Virginia 23298, United States; orcid.org/0000-0002-9536-1743; Email: msafo@vcu.edu

Authors

Piyusha P. Pagare – Department of Medicinal Chemistry, Virginia Commonwealth University, Richmond, Virginia 23298, United States; orcid.org/0000-0002-4848-2673

Mohini S. Ghatge – Department of Medicinal Chemistry and The Institute for Structural Biology, Drug Discovery, and Development, School of Pharmacy, Virginia Commonwealth University, Richmond, Virginia 23298, United States

Qiukan Chen – Division of Hematology, The Children's Hospital of Philadelphia, Philadelphia, Pennsylvania 19104, United States

Faik N. Musayev – Department of Medicinal Chemistry and The Institute for Structural Biology, Drug Discovery, and Development, School of Pharmacy, Virginia Commonwealth University, Richmond, Virginia 23298, United States

Jurgen Venitz – Department of Pharmaceutics, Virginia Commonwealth University, Richmond, Virginia 23298, United States

Osheiza Abdulmalik – Division of Hematology, The Children's Hospital of Philadelphia, Philadelphia, Pennsylvania 19104, United States

Complete contact information is available at: <https://pubs.acs.org/doi/10.1021/acs.jmedchem.0c01287>

Author Contributions

M.K.S. and Y.Z. conceived and oversaw the project and finalized the manuscript. P.P. drafted the manuscript. P.P. conducted the chemical synthesis. P.P. and M.S.G. conducted the in vitro studies with normal human blood. P.P. and F.N.M. conducted the crystallography studies. O.A. designed, conducted, and analyzed in vitro and in vivo biochemical assays and edited the manuscript. Q.C. conducted in vitro antisickling and in vivo studies.

Notes

The authors declare the following competing financial interest(s): Virginia Commonwealth University has filed a patent related to compounds 1-14.

■ ACKNOWLEDGMENTS

This work was supported by NIH/NIMHD grant MD009124 (M.K.S.). Structural biology resources were provided by NIH Shared Instrumentation Grant S10OD021756 (M.K.S.) and Virginia General Assembly Higher Education Equipment Trust Fund (HEETF) to Virginia Commonwealth University (M.K.S.).

■ ABBREVIATIONS

Hb, hemoglobin; SCD, sickle cell disease; HbS, sickle hemoglobin; RBC, red blood cell; HU, hydroxyurea; AEH, allosteric effector of hemoglobin; ALDH, aldehyde dehydrogenase; OEC, oxygen equilibrium curve; SS, homozygous sickle cell trait; HbA, normal hemoglobin; $p\text{O}_2$, partial pressure of oxygen; $p\text{CO}_2$, partial pressure of carbon dioxide; $s\text{O}_2$, oxygen-saturation; H_{ctv} , hematocrit; tHb, total hemoglobin; P_{50} , partial pressure of oxygen at which 50% of hemoglobin is saturated with oxygen

■ REFERENCES

- (1) Pauling, L.; Itano, H. A.; Singer, S. J.; Wells, I. C. Sickle Cell Anemia, a Molecular Disease. *Science* **1949**, *110*, 543–548.
- (2) Cretigny, I.; Edelstein, S. J. Double Strand Packing in Hemoglobin S Fibers. *J. Mol. Biol.* **1993**, *230*, 733–738.
- (3) Ferrone, F. A. Polymerization and Sickle Cell Disease: A Molecular View. *Microcirculation* **2004**, *11*, 115–128.
- (4) Ghatge, M. S.; Ahmed, M. H.; Omar, A. S. M.; Pagare, P. P.; Rosef, S.; Kellogg, G. E.; Abdulmalik, O.; Safo, M. K. Crystal Structure of Carbonmonoxy Sickle Hemoglobin in R-State Conformation. *J. Struct. Biol.* **2016**, *194*, 446–450.
- (5) Rogers, S. C.; Ross, J. G. C.; d'Avignon, A.; Gibbons, L. B.; Gazit, V.; Hassan, M. N.; McLaughlin, D.; Griffin, S.; Neumayr, T.; Debaun, M.; DeBaun, M. R.; Doctor, A. Sickle Hemoglobin Disturbs Normal Coupling among Erythrocyte O₂ Content, Glycolysis, and Antioxidant Capacity. *Blood* **2013**, *121*, 1651–1662.
- (6) Poillon, W. N.; Kim, B. C.; Welty, E. V.; Walder, J. A. The Effect of 2,3-Diphosphoglycerate on the Solubility of Deoxyhemoglobin S. *Arch. Biochem. Biophys.* **1986**, *249*, 301–305.
- (7) Poillon, W.; Kim, B. 2,3-Diphosphoglycerate and Intracellular PH as Interdependent Determinants of the Physiologic Solubility of Deoxyhemoglobin S. *Blood* **1990**, *76*, 1028–1036.
- (8) Jensen, F. B. The Dual Roles of Red Blood Cells in Tissue Oxygen Delivery: Oxygen Carriers and Regulators of Local Blood Flow. *J. Exp. Biol.* **2009**, *212*, 3387–3393.
- (9) Habara, A.; Steinberg, M. H. Minireview: Genetic Basis of Heterogeneity and Severity in Sickle Cell Disease. *Exp. Biol. Med.* **2016**, *241*, 689–696.
- (10) Thein, M. S.; Igbineweka, N. E.; Thein, S. L. Sickle Cell Disease in the Older Adult. *Pathology* **2017**, *49*, 1–9.

- (11) Chaturvedi, S.; DeBaun, M. R. Evolution of Sickle Cell Disease from a Life-Threatening Disease of Children to a Chronic Disease of Adults: The Last 40 Years. *Am. J. Hematol.* **2016**, *91*, 5–14.
- (12) Nagel, R. L.; Johnson, J.; Bookchin, R. M.; Garel, M. C.; Rosa, J.; Schiliro, G.; Wajcman, H.; Labie, D.; Moo-Penn, W.; Castro, O. β -Chain contact sites in the haemoglobin S polymer. *Nature* **1980**, *283*, 832–834.
- (13) Rhoda, M.-D.; Martin, J.; Blouquit, Y.; Garel, M.-C.; Edelstein, S. J.; Rosa, J. Sickle Cell Hemoglobin Fiber Formation Strongly Inhibited by the Stanleyville II Mutation (A78 Asn \rightarrow Lys). *Biochem. Biophys. Res. Commun.* **1983**, *111*, 8–13.
- (14) Benesch, R. E.; Kwong, S.; Edalji, R.; Benesch, R. Alpha Chain Mutations with Opposite Effects on the Gelation of Hemoglobin S. *J. Biol. Chem.* **1979**, *254*, 8169–8172.
- (15) CDC. Data & Statistics on Sickle Cell Disease, CDC <https://www.cdc.gov/ncbddd/sicklecell/data.html> (accessed May 2, 2020).
- (16) Goldberg, M. A.; Brugnara, C.; Dover, G. J.; Schapira, L.; Lacroix, L.; Bunn, H. F. Hydroxyurea and Erythropoietin Therapy in Sickle Cell Anemia. *Semin. Oncol.* **1992**, *19*, 74–81.
- (17) Platt, O. S. Hydroxyurea for the Treatment of Sickle Cell Anemia. *N. Engl. J. Med.* **2008**, *358*, 1362–1369.
- (18) Sinha, C. B.; Bakshi, N.; Ross, D.; Krishnamurti, L. From Trust to Skepticism: An In-Depth Analysis across Age Groups of Adults with Sickle Cell Disease on Their Perspectives Regarding Hydroxyurea. *PLoS One* **2018**, *13*, No. e0199375.
- (19) Niihara, Y.; Zerez, C. R.; Akiyama, D. S.; Tanaka, K. R. Oral L-Glutamine Therapy for Sickle Cell Anemia: I. Subjective Clinical Improvement and Favorable Change in Red Cell NAD Redox Potential. *Am. J. Hematol.* **1998**, *58*, 117–121.
- (20) Kaufman, M. B. Pharmaceutical Approval Update. *P T* **2017**, *42*, 620–621.
- (21) Vichinsky, E.; Hoppe, C. C.; Ataga, K. I.; Ware, R. E.; Nduba, V.; El-Beshlawy, A.; Hassab, H.; Achebe, M. M.; Alkindi, S.; Brown, R. C.; Diuguid, D. L.; Telfer, P.; Tsitsikas, D. A.; Elghandour, A.; Gordeuk, V. R.; Kanter, J.; Abboud, M. R.; Lehrer-Graiwer, J.; Tonda, M.; Intondi, A.; Tong, B.; Howard, J. A Phase 3 Randomized Trial of Voxelotor in Sickle Cell Disease. *N. Engl. J. Med.* **2019**, *381*, 509–519.
- (22) Ataga, K. I.; Kutlar, A.; Kanter, J.; Liles, D.; Cancado, R.; Friedrisch, J.; Guthrie, T. H.; Knight-Madden, J.; Alvarez, O. A.; Gordeuk, V. R.; Gualandro, S.; Colella, M. P.; Smith, W. R.; Rollins, S. A.; Stocker, J. W.; Rother, R. P. Crizanlizumab for the Prevention of Pain Crises in Sickle Cell Disease. *N. Engl. J. Med.* **2017**, *376*, 429–439.
- (23) Ferrone, F. A. GBT440 Increases Haemoglobin Oxygen Affinity, Reduces Sickling and Prolongs RBC Half-Life in a Murine Model of Sickle Cell Disease. *Br. J. Haematol.* **2016**, *174*, 499–500.
- (24) Safo, M. K.; Kato, G. J. Therapeutic Strategies to Alter the Oxygen Affinity of Sickle Hemoglobin. *Hematol. Oncol. Clin. North Am.* **2014**, *28*, 217–231.
- (25) Safo, M. K.; Bruno, S. Allosteric Effectors of Hemoglobin: Past, Present and Future. In *Chemistry and Biochemistry of Oxygen Therapeutics*; Mozzarelli, A., Bettati, S., Eds.; John Wiley & Sons, Ltd.: Chichester, West Sussex, England, 2011; pp 285–300.
- (26) Godfrey, V. B.; Chen, L. J.; Griffin, R. J.; Lebetkin, E. H.; Burka, L. T. Distribution and Metabolism of (5-Hydroxymethyl)Furfural in Male F344 Rats and B6C3F1 Mice after Oral Administration. *J. Toxicol. Environ. Health, Part A* **1999**, *57*, 199–210.
- (27) Vasiliou, V.; Pappa, A.; Petersen, D. R. Role of Aldehyde Dehydrogenases in Endogenous and Xenobiotic Metabolism. *Chem.-Biol. Interact.* **2000**, *129*, 1–19.
- (28) Yoshida, A.; Rzhetsky, A.; Hsu, L. C.; Chang, C. Human Aldehyde Dehydrogenase Gene Family. *Eur. J. Biochem.* **1998**, *251*, 549–557.
- (29) Stern, W.; Mathews, D.; McKew, J.; Shen, X.; Kato, G. J. A Phase I, First-in-Man, Dose-Response Study of Aes-103 (5-HMF), an Anti-Sickling, Allosteric Modifier of Hemoglobin Oxygen Affinity in Healthy Norman Volunteers. *Blood* **2012**, *120*, 3210.
- (30) Parikh, A.; Venitz, J. Novel In vitro Target-site Drug Disposition (TSDD)/Pharmacodynamic (PD) Model for 5-Hydroxymethyl Furfural (5-HMF) in Human Whole Blood.: PII-068. *Clin. Pharmacol. Ther.* **2014**, *95*.
- (31) Pryde, D. C.; Tran, T.-D.; Jones, P.; Duckworth, J.; Howard, M.; Gardner, I.; Hyland, R.; Webster, R.; Wenham, T.; Bagal, S.; Omoto, K.; Schneider, R. P.; Lin, J. Medicinal Chemistry Approaches to Avoid Aldehyde Oxidase Metabolism. *Bioorg. Med. Chem. Lett.* **2012**, *22*, 2856–2860.
- (32) Pryde, D. C.; Dalvie, D.; Hu, Q.; Jones, P.; Obach, R. S.; Tran, T.-D. Aldehyde Oxidase: An Enzyme of Emerging Importance in Drug Discovery. *J. Med. Chem.* **2010**, *53*, 8441–8460.
- (33) Nnamani, I. N.; Joshi, G. S.; Danso-Danquah, R.; Abdulmalik, O.; Asakura, T.; Abraham, D. J.; Safo, M. K. Pyridyl Derivatives of Benzaldehyde as Potential Antisickling Agents. *Chem. Biodiversity* **2008**, *5*, 1762–1769.
- (34) Abdulmalik, O.; Ghatge, M. S.; Musayev, F. N.; Parikh, A.; Chen, Q.; Yang, J.; Nnamani, I.; Danso-Danquah, R.; Eseonu, D. N.; Asakura, T.; Abraham, D. J.; Venitz, J.; Safo, M. K. Crystallographic Analysis of Human Hemoglobin Elucidates the Structural Basis of the Potent and Dual Antisickling Activity of Pyridyl Derivatives of Vanillin. *Acta Crystallogr., Sect. D: Biol. Crystallogr.* **2011**, *67*, 920–928.
- (35) Deshpande, T. M.; Pagare, P. P.; Ghatge, M. S.; Chen, Q.; Musayev, F. N.; Venitz, J.; Zhang, Y.; Abdulmalik, O.; Safo, M. K. Rational Modification of Vanillin Derivatives to Stereospecifically Destabilize Sickle Hemoglobin Polymer Formation. *Acta Crystallogr., Sect. D: Struct. Biol.* **2018**, *74*, 956–964.
- (36) Xu, G. G.; Pagare, P. P.; Ghatge, M. S.; Safo, R. P.; Gazi, A.; Chen, Q.; David, T.; Alabbas, A. B.; Musayev, F. N.; Venitz, J.; Zhang, Y.; Safo, M. K.; Abdulmalik, O. Design, Synthesis, and Biological Evaluation of Ester and Ether Derivatives of Antisickling Agent 5-HMF for the Treatment of Sickle Cell Disease. *Mol. Pharm.* **2017**, *14*, 3499–3511.
- (37) Abdulmalik, O.; Deshpande, T.; Ghatge, M.; Zhang, Y.; Venitz, J.; Parikh, A.; Safo, M. K. Novel Structurally-Modified Allosteric Effectors of Hemoglobin Exhibit Superior Antisickling Properties. *Blood* **2014**, *124*, 218.
- (38) Safo, M. K.; Abdulmalik, O.; Danso-Danquah, R.; Burnett, J. C.; Nokuri, S.; Joshi, G. S.; Musayev, F. N.; Asakura, T.; Abraham, D. J. Structural Basis for the Potent Antisickling Effect of a Novel Class of Five-Membered Heterocyclic Aldehydic Compounds. *J. Med. Chem.* **2004**, *47*, 4665–4676.
- (39) Pagare, P. P.; Ghatge, M. S.; Musayev, F. N.; Deshpande, T. M.; Chen, Q.; Braxton, C.; Kim, S.; Venitz, J.; Zhang, Y.; Abdulmalik, O.; Safo, M. K. Rational Design of Pyridyl Derivatives of Vanillin for the Treatment of Sickle Cell Disease. *Bioorg. Med. Chem.* **2018**, *26*, 2530–2538.
- (40) Abraham, D.; Mehanna, A.; Wireko, F.; Whitney, J.; Thomas, R.; Orringer, E. Vanillin, a Potential Agent for the Treatment of Sickle Cell Anemia. *Blood* **1991**, *77*, 1334–1341.
- (41) Abdulmalik, O.; Safo, M. K.; Chen, Q.; Yang, J.; Brugnara, C.; Ohene-Frempong, K.; Abraham, D. J.; Asakura, T. 5-Hydroxymethyl-2-Furfural Modifies Intracellular Sickle Haemoglobin and Inhibits Sickling of Red Blood Cells. *Br. J. Haematol.* **2005**, *128*, 552–561.
- (42) ASCO Post Staff. *FDA Approves Voxelotor for Sickle Cell Disease*; FDA, 2019.
- (43) Metcalf, B.; Chuang, C.; Dufu, K.; Patel, M. P.; Silva-Garcia, A.; Johnson, C.; Lu, Q.; Partridge, J. R.; Patskovska, L.; Patskovsky, Y.; Almo, S. C.; Jacobson, M. P.; Hua, L.; Xu, Q.; Gwaltney, S. L.; Yee, C.; Harris, J.; Morgan, B. P.; James, J.; Xu, D.; Hutchaleelaha, A.; Paulvannan, K.; Oksenberg, D.; Li, Z. Discovery of GBT440, an Orally Bioavailable R-State Stabilizer of Sickle Cell Hemoglobin. *ACS Med. Chem. Lett.* **2017**, *8*, 321–326.
- (44) Wireko, F. C.; Abraham, D. J. X-Ray Diffraction Study of the Binding of the Antisickling Agent 12C79 to Human Hemoglobin. *Proc. Natl. Acad. Sci. U.S.A.* **1991**, *88*, 2209–2211.
- (45) Safo, M. K.; Ahmed, M. H.; Ghatge, M. S.; Boyiri, T. Hemoglobin-Ligand Binding: Understanding Hb Function and Allostery on Atomic Level. *Biochim. Biophys. Acta* **2011**, *1814*, 797–809.

- (46) Jenkins, J. D.; Musayev, F. N.; Danso-Danquah, R.; Abraham, D. J.; Safo, M. K. Structure of Relaxed-State Human Hemoglobin: Insight into Ligand Uptake, Transport and Release. *Acta Crystallogr., Sect. D: Biol. Crystallogr.* **2009**, *65*, 41–48.
- (47) Silva, M. M.; Rogers, P. H.; Arnone, A. A Third Quaternary Structure of Human Hemoglobin A at 1.7 Å Resolution. *J. Biol. Chem.* **1992**, *267*, 17248–17256.
- (48) Perutz, M. F. Nature of Haem-Haem Interaction. *Nature* **1972**, *237*, 495–499.
- (49) Perutz, M. F. Hemoglobin Structure and Respiratory Transport. *Sci. Am.* **1978**, *239*, 92–125.
- (50) Perutz, M. F.; Wilkinson, A. J.; Paoli, M.; Dodson, G. G. The Stereochemical Mechanism of the Cooperative Effects in Hemoglobin Revisited. *Annu. Rev. Biophys. Biomol. Struct.* **1998**, *27*, 1–34.
- (51) Beddell, C. R.; Goodford, P. J.; Kneen, G.; White, R. D.; Wilkinson, S.; Wootton, R. Substituted Benzaldehydes Designed to Increase the Oxygen Affinity of Human Haemoglobin and Inhibit the Sickling of Sickle Erythrocytes. *Br. J. Pharmacol.* **1984**, *82*, 397–407.
- (52) Oksenberg, D.; Dufu, K.; Patel, M. P.; Chuang, C.; Li, Z.; Xu, Q.; Silva-Garcia, A.; Zhou, C.; Hutchaleelaha, A.; Patskovska, L.; Patskovsky, Y.; Almo, S. C.; Sinha, U.; Metcalf, B. W.; Archer, D. R. GBT440 Increases Haemoglobin Oxygen Affinity, Reduces Sickling and Prolongs RBC Half-Life in a Murine Model of Sickle Cell Disease. *Br. J. Haematol.* **2016**, *175*, 141–153.
- (53) Echols, N.; Grosse-Kunstleve, R. W.; Afonine, P. V.; Bunkóczi, G.; Chen, V. B.; Headd, J. J.; McCoy, A. J.; Moriarty, N. W.; Read, R. J.; Richardson, D. C.; Richardson, J. S.; Terwilliger, T. C.; Adams, P. D. Graphical Tools for Macromolecular Crystallography in PHENIX. *J. Appl. Crystallogr.* **2012**, *45*, 581–586.
- (54) Brünger, A. T.; Adams, P. D.; Clore, G. M.; DeLano, W. L.; Gros, P.; Grosse-Kunstleve, R. W.; Jiang, J. S.; Kuszewski, J.; Nilges, M.; Pannu, N. S.; Read, R. J.; Rice, L. M.; Simonson, T.; Warren, G. L. Crystallography & NMR System: A New Software Suite for Macromolecular Structure Determination. *Acta Crystallogr., Sect. D: Biol. Crystallogr.* **1998**, *54*, 905–921.
- (55) Emsley, P.; Lohkamp, B.; Scott, W. G.; Cowtan, K. Features and Development of Coot. *Acta Crystallogr., Sect. D: Biol. Crystallogr.* **2010**, *66*, 486–501.
- (56) Kato, G. J. New Insights into Sickle Cell Disease: Mechanisms and Investigational Therapies. *Curr. Opin. Hematol.* **2016**, *23*, 224–232.
- (57) Drewry, J. A.; Fletcher, S.; Hassan, H.; Gunning, P. T. Novel Asymmetrically Functionalized Bis-Dipicolylamine Metal Complexes: Peripheral Decoration of a Potent Anion Recognition Scaffold. *Org. Biomol. Chem.* **2009**, *7*, 5074–5077.
- (58) De, L. S.; Liu, W.; Lo, H. Y.; Nemoto, P. A. Benzimidazole Inhibitors of Leukotriene Production. WO2012061169A1, Oct 5, 2012.
- (59) Zhang, D.; Bousquet, B.; Mulatier, J.-C.; Pitrat, D.; Jean, M.; Vanthuyne, N.; Guy, L.; Dutasta, J.-P.; Martinez, A. Synthesis, Resolution, and Absolute Configuration of Chiral Tris(2-Pyridylmethyl)Amine-Based Hemicyclopentane Molecular Cages. *J. Org. Chem.* **2017**, *82*, 6082–6088.
- (60) Cheng, L.; Schell, P. Isoxazol-3(2h)-One Analogs as Plasminogen Inhibitors and Their Use in the Treatment of Fibrinolysis Related Diseases. WO2012047156A1, Dec 4, 2012.
- (61) Gaillard, P.; Seenisamy, J.; Liu-Bujalski, L.; Caldwell, R. D.; Potnick, J.; Qiu, H.; Neagu, C.; Jones, R.; Won, A. C.; Goutopoulos, A.; Sherer, B.; Johnson, T. L.; Gardberg, A. Heteroaryl Compounds as Btk Inhibitors and Uses Thereof. U.S. Patent 2,016,096,834 A1, Oct 6, 2015.
- (62) Safo, M. K.; Abraham, D. J. X-ray Crystallography of Hemoglobins. *Hemoglobin Disorders; Methods in Molecular Biology*; Humana Press, Totowa, NJ, USA, 2003; pp 1–19.
- (63) Winn, M. D.; Ballard, C. C.; Cowtan, K. D.; Dodson, E. J.; Emsley, P.; Evans, P. R.; Keegan, R. M.; Krissinel, E. B.; Leslie, A. G. W.; McCoy, A.; McNicholas, S. J.; Murshudov, G. N.; Pannu, N. S.; Potterton, E. A.; Powell, H. R.; Read, R. J.; Vagin, A.; Wilson, K. S. Overview of the CCP4 suite and current developments. *Acta Crystallogr., Sect. D: Biol. Crystallogr.* **2011**, *67*, 235–242.
- (64) Adams, P. D.; Afonine, P. V.; Bunkóczi, G.; Chen, V. B.; Echols, N.; Headd, J. J.; Hung, L.-W.; Jain, S.; Kapral, G. J.; Grosse Kunstleve, R. W.; McCoy, A. J.; Moriarty, N. W.; Oeffner, R. D.; Read, R. J.; Richardson, D. C.; Richardson, J. S.; Terwilliger, T. C.; Zwart, P. H. The Phenix Software for Automated Determination of Macromolecular Structures. *Methods* **2011**, *55*, 94–106.